eNeuro

Research Article: New Research | Disorders of the Nervous System

Dynamic and Sex-Specific Changes in Gonadotropin-Releasing Hormone Neuron Activity and Excitability in a Mouse Model of Temporal Lobe Epilepsy

Jiang Li[1], Jordyn A. Robare[2], Liying Gao[3], M. Amin Ghane[2], Jodi A. Flaws[3], Mark E. Nelson[1,2,4] and Catherine A. Christian[1,2,4]

[1]*Neuroscience Program, University of Illinois at Urbana-Champaign, Urbana, Illinois, 61801, USA*

[2]*Department of Molecular & Integrative Physiology, University of Illinois at Urbana-Champaign, Urbana, Illinois, 61801, USA*

[3]*Department of Comparative Biosciences, University of Illinois at Urbana-Champaign, Urbana, Illinois, 61801, USA*

[4]*Beckman Institute for Advanced Science and Technology, University of Illinois at Urbana-Champaign, Urbana, Illinois, 61801, USA*

DOI: 10.1523/ENEURO.0273-18.2018

Received: 9 July 2018

Revised: 4 September 2018

Accepted: 5 September 2018

Published: 11 September 2018

Funding: http://doi.org/10.13039/100000065HHS | NIH | National Institute of Neurological Disorders and Stroke (NINDS)
R01 NS105825
R03 NS103029

Funding: http://doi.org/10.13039/100005302UofI | University of Illinois at Urbana-Champaign (UIUC)
Startup Funds

Funding: http://doi.org/10.13039/100005471Beckman Institute for Advanced Science and Technology, University of Illinois, Urbana-Champaign
Graduate Fellowship

J.L. and C.A.C. designed research; J.L., J.A.R., L.G., M.A.G., and J.A.F. performed research; J.L., M.E.N., and C.A.C. analyzed data; J.L. and C.A.C. wrote the paper.

Corresponding author: cathchri@illinois.edu

Cite as: eNeuro 2018; 10.1523/ENEURO.0273-18.2018

Manuscript Title Page

1. Manuscript Title Dynamic and Sex-Specific Changes in Gonadotropin-Releasing Hormone Neuron Activity and Excitability in a Mouse Model of Temporal Lobe Epilepsy

2. Abbreviated Title Altered GnRH neuron function in mouse model of TLE

3. Author Names and Affiliations

Jiang Li[1], Jordyn A. Robare[2], Liying Gao[3], M. Amin Ghane[2], Jodi A. Flaws[3], Mark E. Nelson[1,2,4], and Catherine A. Christian[1,2,4]

[1]Neuroscience Program, [2]Department of Molecular & Integrative Physiology, [3]Department of Comparative Biosciences, [4]Beckman Institute for Advanced Science and Technology, University of Illinois at Urbana-Champaign, Urbana, Illinois, 61801, USA

4. Author Contributions: JL and CAC designed research; JL, JAR, LG, MAG, and JAF performed research; JL, MEN, and CAC analyzed data; JL and CAC wrote the paper

5. Correspondence should be addressed to (include email address) Catherine A. Christian, University of Illinois at Urbana-Champaign, 506 S. Mathews Ave., 523 Medical Sciences Building, Urbana, Illinois 61801, USA; Phone (217) 244-8230; Email: cathchri@illinois.edu

6. Number of Figures 9
7. Number of Tables 4
8. Number of Multimedia 0
9. Number of words for Abstract 249
10. Number of words for Significance Statement 120
11. Number of words for Introduction 691
12. Number of words for Discussion 2600

13. Acknowledgements

This work was supported by National Institutes of Health/National Institute of Neurological Disorders and Stroke (NIH/NINDS) grants R01 NS105825 and R03 NS103029 (CAC), startup funds from the University of Illinois at Urbana-Champaign (CAC), and a Beckman Institute Graduate Fellowship (JL). We thank Jae Seong Kim for assistance with stereotaxic injections; Lillian Scanlon, Vincent Abejuela, Jason Lamano, and Shivang Chaudhary for assistance with estrous cycle monitoring and seizure video screening; Rana Youssef for assistance with histology; Justin Rhodes for assistance with logistic regression analysis; and Daniel Llano for helpful editorial comments.

14. Conflict of Interest

A. No The authors declare no competing financial interests.

15. Funding sources NIH/NINDS, University of Illinois at Urbana-Champaign, Beckman Institute

Abstract

Reproductive endocrine disorders are prominent co-morbidities of temporal lobe epilepsy (TLE) in both men and women. The neural mechanisms underlying these co-morbidities remain unclear, but hypothalamic gonadotropin-releasing hormone (GnRH) neurons may be involved. Here we report the first direct demonstrations of aberrant GnRH neuron function in an animal model of epilepsy. Recordings of GnRH neuron firing and excitability were made in acute mouse brain slices prepared 2 months after intrahippocampal injection of kainate (KA) or control saline, a well-established TLE model in which most females develop co-morbid estrous cycle disruption. GnRH neurons from control females showed elevated firing and excitability on estrus compared with diestrus. By contrast, cells from KA-injected females that developed prolonged, disrupted estrous cycles (KA-long) showed the reverse pattern. Firing rates of cells from KA-injected females that maintained regular cycles (KA-regular) were not different from controls on diestrus, but were reduced on estrus. In KA-injected males, only GnRH neurons in the medial septum displayed elevated firing. In contrast to the diestrus-vs.-estrus and sex-specific changes in firing, GnRH neuron intrinsic excitability was elevated in all KA-injected groups, indicating a role for afferent synaptic and neuromodulatory inputs in shaping overall changes in firing activity. Furthermore, KA-injected females showed cycle-stage-specific changes in circulating sex steroids on diestrus and estrus that also differed between KA-long and KA-regular groups. Together, these findings reveal that the effects of epilepsy on the neural control of reproduction are dynamic across the estrous cycle, distinct in association with co-morbid estrous cycle disruption severity, and sex-specific.

62 **Significance Statement**

63 People with epilepsy are at higher risk of reproductive endocrine disorders compared
64 with the general population, but the neural mechanisms linking epilepsy and these co-
65 morbidities are unknown. Here we report changes in the function of gonadotropin-releasing
66 hormone (GnRH) neurons, which control fertility, in a mouse model of temporal lobe epilepsy.
67 GnRH neurons from epileptic female mice showed changes in activity dependent on estrous
68 cycle stage and associated with severity of cycle disruption. The impacts of epilepsy on GnRH
69 neurons in males were less severe. These findings provide novel evidence for impacts of
70 epilepsy on GnRH neuron function, and will thus be of clinical relevance in developing new
71 strategies to ameliorate reproductive co-morbidities and to treat the underlying seizures and
72 epilepsy.

73

74

Introduction

Reproductive endocrine disorders are prominent co-morbidities of epilepsy (Herzog et al., 1986a, b; Bilo et al., 2001; Klein et al., 2001; Löfgren et al., 2007; Bauer and Cooper-Mahkorn, 2008). For example, 10-20% of women with epilepsy develop polycystic ovary syndrome, in comparison to 5% of women without epilepsy (Bauer et al., 2000; Herzog, 2008). Disrupted menstrual cycle intervals and amenorrhea are also commonly observed (Herzog et al., 2003; Herzog, 2008; Zhou et al., 2012). Furthermore, semen abnormalities are reported in up to 90% of men with epilepsy (Herzog, 2008), and 10-30% of men with focal epilepsy develop low serum testosterone levels (Talbot et al., 2008). The neural mechanisms linking epilepsy to co-morbid reproductive endocrine disorders are unknown.

Temporal lobe epilepsy (TLE) is the most common focal epilepsy in patients of reproductive age (Engel, 2001). Roughly 60% of women with TLE not taking antiepileptic drugs exhibit menstrual disorders, indicating that there is a strong association between TLE seizures and reproductive endocrine dysfunction (Herzog et al., 1986a). Furthermore, seizures are exacerbated at certain phases of the menstrual cycle in approximately 40% of women with epilepsy, a pattern termed catamenial epilepsy (Laidlaw, 1956; Herzog et al., 2004). One major type of catamenial epilepsy is characterized by a prolonged period of elevated seizure susceptibility and seizure clustering associated with an inadequate luteal phase within irregular, anovulatory menstrual cycles (Herzog et al., 1997). Therefore, seizure control through the restoration of proper reproductive cyclicity could be a novel therapeutic approach for many women with epilepsy. Understanding the mechanisms underlying epilepsy-induced

reproductive endocrine disorders is crucial for the development of new strategies for both reproductive cycle maintenance and seizure management.

The hypothalamic gonadotropin-releasing hormone (GnRH) neurons are the final neural output driving the activity of downstream elements of the hypothalamic-pituitary-gonadal (HPG) axis (Herbison, 2006; Christian, 2017). Because of the difficulty in measuring GnRH directly, luteinizing hormone (LH) is often used as a readout of GnRH secretion; pituitary gonadotrophs secrete bolus pulses of LH in response to pulsatile GnRH stimulation. Altered LH pulse frequency has been reported in both men and women with epilepsy (Herzog et al., 1990; Drislane et al., 1994; Quigg et al., 2002), suggesting epilepsy-induced changes in GnRH release. To date, studies of the impacts of epilepsy on GnRH neurons have been limited to anatomical analysis of GnRH immunoreactivity in animal models, with conflicting results (Amado et al., 1993; Friedman et al., 2002; Fawley et al., 2012). Whether GnRH neuron function is impaired in epilepsy has not been tested directly. Furthermore, it is unknown whether the impacts of epilepsy on GnRH neurons vary with the female reproductive cycle, or are different between males and females.

Multiple rodent models of TLE display disrupted estrous cycles (Amado et al., 1987; Edwards et al., 1999; Scharfman et al., 2008), including the intrahippocampal kainate (KA) mouse model (Li et al., 2017). Here, we studied the impacts of epilepsy on GnRH neuron function in this model of TLE. We assessed the spontaneous firing rate and intrinsic excitability of GnRH neurons in brain slices obtained from females (on diestrus and estrus) and males ~2 months after intrahippocampal injection of KA or control saline. Diestrus and estrus were chosen for examination as these stages are associated with changes in seizure susceptibility in

rodents (Finn and Gee, 1994; Maguire et al., 2005) and show the greatest degree of change in this model of TLE (Li et al., 2017). Periodic burst firing may underlie GnRH secretion (Kelly and Wagner, 2002). Therefore, we also analyzed the burst properties of the recorded GnRH neurons. Sex steroids exert potent feedback on GnRH neuron activity (Pielecka et al., 2006; Moenter et al., 2009), and altered serum sex steroid levels were reported in other rodent models of epilepsy (Amado et al., 1987; Amado and Cavalheiro, 1998; Edwards et al., 2000; Scharfman et al., 2008). Therefore, we measured serum progesterone (P_4) and estradiol (E_2) in control and KA-injected females, and testosterone (T) in males. Our results indicate that the effects of intrahippocampal KA injection on GnRH neuron activity and excitability are different on diestrus compared with estrus, varied according to the severity of co-morbid estrous cycle disruption, and sex-specific.

Materials and Methods

Animals. All animal procedures were approved by the Institutional Animal Care and Use Committee of the University of Illinois at Urbana-Champaign. GnRH-tdTomato transgenic mice were bred by crossing GnRH-Cre$^+$ females (Yoon et al., 2005) (Jackson Labs #021207) and Ai9 males (Madisen et al., 2010) (Jackson Labs #007909). Both strains are on the C57BL/6J background. Mice were housed in a standard environment in a 14:10 h light:dark cycle (7:00 P.M. lights off) to promote breeding and estrous cyclicity (Fox et al., 2006), with up to five mice per cage. Genotyping to identify pups expressing the Cre allele was done by PCR of DNA extracted from tail clips collected prior to postnatal day (P) 21 using the following 4 primer sequences as suggested by Jackson Labs: 1) transgene reverse CGG ACA GAA GCA TTT TCC AG; 2)

transgene forward ACA GGT GTC TGT CCC ATG TCT; 3) internal positive control forward CAA ATG TTG CTT GTC TGG TG; 4) internal positive control reverse GTC AGT CGA GTG CAC AGT TT.

Estrous Cycle Monitoring. A regular mouse estrous cycle is typically 4-5 days long (Byers et al., 2012). Because mouse estrous cycles can be disrupted easily by environmental or other stressors, we categorized cycles up to 6 d in length as "regular" to account for minor temporal disruption and to minimize false positives of estrous cycle disruption. To confirm that all female mice had regular estrous cycles, daily vaginal smears were performed between 10:00 AM and 12:00 PM starting on or after P42. 20 μl of sterile PBS was gently inserted into the vaginal cavity using a 100-200 μl sterile pipette tip, quickly withdrawn, and examined on a microscope slide by brightfield microscopy. Regular estrous cycles were defined as at least 2 cycles 4-6 d in length with proestrus, estrus, metestrus, and diestrus I/II stages occurring in chronological order. Smears were classified into each stage based on the following criteria: 1) proestrus: dominated by nucleated epithelial cells; 2) estrus: dominated by cornified epithelial cells; 3) metestrus: both cornified epithelial cells and leukocytes; 4) diestrus I: dominated by leukocytes; 5) diestrus II: few or no cells present. Mice that did not display regular estrous cycles within 3 weeks of monitoring were excluded from further study.

After intrahippocampal injection of either saline or KA, mice were allowed to rest undisturbed for 1 month to minimize stress and avoid disruption of epileptogenesis. Daily estrous cycle monitoring was then performed until the time of brain slice preparation. The vaginal smears from KA-injected females did not show major changes in smear cytology

161 characteristics. Therefore, the same criteria were used to classify estrous cycle stages for all
162 mice. To promote cyclicity both before and after saline/KA injection, soiled bedding from cages
163 housing male mice was introduced to cages housing females when irregular cyclicity was noted.
164 The average cycle length used to categorize KA-injected mice as "KA-long" (i.e., estrous cycle
165 period $\geq$7 d) or "KA-regular" was calculated from the daily monitoring for the time from 42 days
166 after injection to the day of brain slice preparation. Cycle period was chosen as the primary
167 parameter for characterization because elongation of the estrous cycle is a prominent feature
168 of cycle disruption in this model of TLE (Li et al., 2017).

169

170 *Intrahippocampal Injections.* Stereotaxic injections in mice 8 weeks of age and older were
171 performed under 2-3% oxygen-vaporized isoflurane anesthesia (Clipper Distributing Company,
172 St. Joseph, MO). KA (Tocris Bioscience, Bristol, United Kingdom; 50 nl of 20 mM prepared in 0.9%
173 sterile saline) was injected into the right dorsal hippocampal CA1 region (coordinates: 1.8 mm
174 posterior and 1.5 mm lateral to Bregma; 1.5 mm ventral to the cortical surface). Control mice
175 were injected with an equivalent volume of sterile saline. Carprofen (5 mg/kg, Zoetis,
176 Kalamazoo, MI) was administered s.c. at the beginning of surgery for analgesia. After closing
177 the scalp incision with sutures, anesthetic 2.5% lidocaine + 2.5% prilocaine cream (Hi-Tech
178 Pharmacal, Amityville, NY) and Neosporin antibiotic gel (Johnson and Johnson, Skillman, NJ)
179 were applied to the wound.

180

181 *Video Monitoring of Acute Seizures.* After intrahippocampal injection surgery was completed,
182 mice were placed in a transparent and warmed recovery chamber. All KA-injected mice were
183 video monitored to screen for the development of acute seizures within 5 hours after unilateral
184 KA injection. Behavioral seizures of Racine stage 3 (forelimb clonus) and higher (rearing and
185 falling) could be distinguished through the video, whereas behavioral seizures below stage 3
186 (slight head nodding and facial muscle contraction) could not. Freezing or continuous back-
187 circling behaviors indicating nonconvulsive status epilepticus, as previously reported in this
188 model (Bouilleret et al., 1999; Riban et al., 2002), were also noted.

189

190 *Brain Slice Preparation.* Acute brain slices were prepared ~2 months after saline/KA injection.
191 All mice were euthanized by decapitation between 10:00 to 11:00 AM. 300-µm coronal brain
192 sections were prepared using a Leica VT1200S (Leica Biosystems, Buffalo Grove, IL) vibrating
193 blade microtome. Brain slices were bathed in oxygenated (95% O_2, 5% CO_2) ice-cold sucrose
194 solution (containing in mM: 2.5 KCl, 1.25 NaH_2PO_4, 10 $MgSO_4$, 0.5 $CaCl_2$, 11 glucose, 234 sucrose)
195 during sectioning and then transferred to oxygenated artificial cerebrospinal fluid (ACSF) for 30
196 min at 32°C before being transferred to room temperature for at least 30 min. ACSF contained
197 (in mM) 2.5 KCl, 10 glucose, 126 NaCl, 1.25 NaH_2PO_4, 1 $MgSO_4$, 0.5 $CaCl_2$, 26 $NaHCO_3$,
198 osmolarity = ~298 mOsm. For recording, individual slices were placed in a recording chamber
199 on the stage of an upright BX51WI microscope (Olympus America, Center Valley, PA).
200 Oxygenated bath ACSF was warmed to 30-32°C using an inline heater (Warner Instruments,
201 Hamden, CT) and pumped through the slice chamber at a flow rate of 2.5 ml/min.

202 *Targeted Extracellular Recordings.* Targeted extracellular (loose patch) recordings (Nunemaker
203 et al., 2002; Christian et al., 2005) were performed between 11:00 A.M. and 3:00 P.M. for 40-90
204 min/cell to detect spontaneous firing activity. Thick-walled borosilicate glass recording pipettes
205 (~2 MΩ tip resistance) were prepared using a P-1000 electrode puller (Sutter Instruments,
206 Novato, CA) and filled with filtered ACSF solution with 10 mM HEPES buffer added. GnRH
207 neurons expressing tdTomato red fluorescence were identified by brief illumination at 593 nm
208 and targeted for recording under differential infrared contrast optics using an sCMOS camera
209 (Orca-Flash 4.0LT, Hamamatsu Photonics, Japan). Seal resistance was measured at least every
210 30 min. The initial seal resistances ranged from 3.2 to 12 MΩ and the maximum seal resistance
211 was 45 MΩ. Recordings were performed in voltage-clamp mode with the holding potential at 0
212 mV and Bessel-filtered at 12 kHz. No more than three cells were recorded per animal. If a cell
213 displayed no action currents within 1 h of recording, 15 mM KCl was bath-applied to induce
214 firing and confirm successful recording. A picture of the pipette tip position was captured using
215 HCImage software (Hamamatsu) after every recording for neuron location analysis.
216 Classification of soma position in the medial septum (MS), preoptic area (POA), or anterior
217 hypothalamic area (AHA) was based on a mouse brain atlas (Paxinos and Franklin, 2012)
218 (corresponding plates: MS = 23-25, POA = 25-28, AHA = 29). Data acquisition was performed
219 with a MultiClamp 700B amplifier, Digidata 1550 digitizer, and Clampex 10 software (Molecular
220 Devices, Sunnyvale, CA). Action current detection was performed using Clampfit 10.6.

221

222 *Current-Clamp Recordings.* Recordings were performed in the presence of ionotropic GABA and
223 glutamate receptor blockers added to the bath solution (5 µM APV + 20 µM DNQX + 100 µM

picrotoxin, Abcam, Cambridge, MA). Recording pipettes (3-5 MΩ) were filled with a pipette internal solution containing (in mM) 125 K-gluconate, 20 KCl, 10 HEPES, 4 EGTA, 4 Mg-ATP, 0.4 Na-GTP, 0.1 $CaCl_2$, pH = 7.2, osmolarity = 290 mOsm. After achieving the whole-cell configuration using conventional procedures, a 5-mV depolarizing step from -70 mV holding potential was delivered in voltage-clamp mode to measure series and input resistances. Only recordings with series resistance <20 MΩ and input resistance >500 MΩ were included in analyses. Resting membrane potential was maintained near -73 mV (calculated after correction for a 13-mV liquid junction potential) by applying injected current as needed. All recordings were made in bridge-balanced mode. Data acquisition was performed as for targeted extracellular recordings. Data analysis was performed in Clampfit 10.6 for all parameters except action potential threshold, which was determined in MATLAB (MathWorks, Natick, MA) from the value on the phase plot where the dV/dt was $\geq$5 V/s. The area under the F-I curve for each neuron was calculated by a trapezoidal method.

Firing Pattern Categorization and Burst Analysis. Spike train and burst detection analyses were performed in MATLAB. Firing patterns from targeted extracellular recordings were analyzed by constructing an interspike interval (ISI) joint scatter plot, which used the log ISI before (X-axis, logISIn) and after (Y-axis, logISIn+1) a spike to reveal the temporal relationship of neural spikes (Ramcharan et al., 2000; Dodla and Wilson, 2010). For group comparisons of burst properties, 100 bursts were randomly selected from each neuron to construct cumulative probability distributions. For recordings with fewer than 100 bursts, all detected bursts were used.

Code Accessibility. The code used for GnRH neuron firing pattern recognition, burst detection, burst properties analysis, and statistical comparisons of burst activities is available on Github (https://github.com/ChristianLabUIUC/BurstAnalysis). The same files are also available as Extended Data.

Cresyl Violet and GFAP Staining of Hippocampus. At the conclusion of brain slice preparation, the remaining portion of cerebrum containing the hippocampus was collected, fixed in 4% PFA for 24 h at 4^{O}C, and preserved in 30% sucrose solution with 0.5% sodium azide at 4^{O}C until sectioning. 50 µm coronal hippocampal sections were prepared using a freezing microtome (SM 2010R, Leica Biosystems, Buffalo Grove, IL). 4-8 sections per mouse from the dorsal hippocampal region were used for verification of hippocampal sclerosis by Cresyl Violet staining and gliosis by GFAP staining. For Cresyl Violet staining, sections were mounted on charged glass slides, stained with Cresyl Violet (Sigma C5042, St. Louis, MO) for 12 min at room temperature (~22^{O}C), dehydrated with graded ethanol solutions (70%-100%), and cleaned in xylene. For glial fibrillary acidic protein (GFAP) immunostaining, floating sections were incubated in an anti-GFAP mouse monoclonal antibody (1:1000, Sigma G3893) for 48 h at 4^{O}C on a shaker, followed by incubation in Fluorescein horse anti-mouse secondary antibody (1:1000, Vector Laboratories FI-2000, Burlingame, CA) for 2 h at room temperature on a shaker. Sections were then mounted on charged glass slides and coverslipped using Vectashield Hardset Antifade Mounting Medium with DAPI (Vector Laboratories H-1500). Image acquisition was performed using a BX43 light and fluorescence microscope (Olympus) equipped with a Q-Color 3 camera and QCapture 6 software (QImaging, Surrey, British Columbia, Canada).

Hormone Assays. Trunk blood samples from mice used for *in vitro* recordings (n=85 mice) were collected at the time of brain slice preparation. Samples from mice not used for recordings (n=12 mice) were collected after decapitation to replace samples from recorded mice that were contaminated or otherwise unsuitable for analysis. The blood samples were kept at room temperature (~22^{O}C) for 20 min and then on ice for 20 min, followed by centrifugation at room temperature for 15 min. Serum was withdrawn after centrifugation and stored at -20°C until use. Enzyme-linked immunosorbent assays (ELISAs; P_4: DRG Diagnostics, Marburg, Germany; E_2: Calbiotech, Spring Valley, CA; T: IBL America, Minneapolis, MN) were performed according to the manufacturers' instructions. Some samples were diluted to match the volume required for the testing. Samples were run in duplicate and the average of the duplicate was used as the final hormone concentration value for each mouse.

Experimental Design and Statistics. The experimental design is outlined in **Figure 1**. Pre-injection estrous cycle monitoring for adult female mice started on or after P42. Age-matched female and male mice were stereotaxically injected with saline or KA in the dorsal hippocampus. Two months after injection, acute brain slices were prepared and GnRH neuron firing rate and excitability were measured via single-cell electrophysiological recordings. For female mice, recordings were performed on the days of diestrus or estrus. At the time of brain slice preparation, trunk blood serum and hippocampal tissue were collected for hormone analysis and histology, respectively.

Statistical comparisons were made using OriginPro (OriginLab, Northampton, MA), SPSS (IBM, Armonk, NY), or R software. Comparisons between two groups (e.g., diestrus vs. estrus within each treatment group, and saline vs. KA for males) were made using t-tests or Mann-Whitney tests depending on the normality of the data, which was determined using Shapiro Wilk tests. Comparisons between saline, KA-long, and KA-regular females were made separately for diestrus and estrus using Kruskal-Wallis and Dunn's *post hoc* tests or one-way ANOVA and Bonferroni *post hoc* tests based on the normality and the homogeneity of variance within each group as assessed by Shapiro-Wilk tests and Levene's tests, respectively. Data for evoked firing rate and excitability parameters were Box-Cox transformed to achieve normal distributions, and analyzed using three-way ANOVA and Fisher's LSD *post hoc* tests. Comparisons of P_4 and E_2 levels between saline, KA-long, and KA-regular groups at each cycle stage were made using one-way ANOVA and Fisher *post hoc* tests; non-normally distributed data were normalized by log-transformation before analysis. Results in the above tests are reported as means $\pm$ SEM. Firing patterns of GnRH neurons from female mice were assessed using a logistic regression with treatment group (saline, KA-long, and KA-regular) and estrous cycle stage (diestrus and estrus) as factors. The probabilities of neurons displaying bursting, irregular, tonic, or quiet firing patterns were analyzed separately using Fisher's exact tests. Comparisons were made between treatment groups within diestrus or estrus, or within treatment groups between diestrus and estrus. Chi-square tests were used to compare the proportions of GnRH neurons from control and KA-injected male mice that showed bursting and irregular firing patterns, and to compare the proportions of KA-long and KA-regular mice showing hippocampal sclerosis. Correlation analysis was performed using Spearman's Rank-Order tests. Statistical significance in the above

statistical tests was set at $p<0.05$. Cumulative probability distributions were compared using Kolmogorov–Smirnov goodness-of-fit tests, and the criterion for statistical significance in these tests was $p<0.001$.

Results

Confirmation of Hippocampal KA Injection Targeting. Mice treated with intrahippocampal KA exhibit acute non-convulsive or mild clonic status epilepticus followed (within 2 weeks to 2 months) by spontaneous focal seizures that rarely generalize to tonic-clonic seizures, along with histopathological features including hippocampal sclerosis and gliosis, recapitulating cardinal hallmarks of human TLE (Bouilleret et al., 1999; Riban et al., 2002; Blümcke et al., 2013). In these studies, we applied three steps of verification to check the accuracy of intrahippocampal injections: 1) video screening of seizures immediately after KA injection; 2) histopathological assessment of hippocampal sclerosis by Cresyl Violet (Nissl) staining; and 3) immunofluorescent GFAP staining for gliosis. The small subset of mice that were used for trunk blood collection only, without *in vitro* recordings, all displayed acute seizures following KA injection. Therefore, hippocampal tissue used for histology was collected on the day of brain slice preparation for *in vitro* recordings (~ 2 months after injection).

The large majority of KA-injected female mice (57 of 69, 83%) showed at least two seizures within 5 hours after KA injection, and 5 mice showed one seizure. Of the remaining 7 mice, 3 stayed frozen or exhibited backwards circling over the entire recording, 1 mouse did not show seizures or frozen/backwards circling behavior after KA injection, and 3 were not

successfully video recorded (**Table 1**). 4 of these 7 mice displayed prominent granule cell dispersion and other signs of sclerosis in Cresyl Violet staining, as shown in the example in **Figure 2A**. Hippocampi that showed no obvious signs of sclerosis were subsequently evaluated for GFAP staining. In 2 of the remaining 3 mice examined, gliosis was observed in the dentate gyrus and/or CA regions in the injected hippocampus, as shown in the example in **Figure 2B**. The remaining KA-injected female, which did not show acute seizures, hippocampal sclerosis, nor gliosis, was excluded from the final dataset. No signs of sclerosis or gliosis were observed in the dentate gyrus or CA regions collected from randomly selected saline-injected mice (**Figure 2C**). Neither gliosis nor hippocampal sclerosis were observed in the contralateral hippocampus.

Video screening of 13 KA-injected males confirmed that 10 (77%) showed at least 2 seizures (**Table 1**). The remaining 3 mice did not show any behavioral seizures but were confirmed to have developed hippocampal sclerosis by 2 months after injection. Two other male mice were not successfully video recorded, but were confirmed by Cresyl Violet staining to have developed hippocampal sclerosis.

Rate of Development of Hippocampal Sclerosis Does Not Correlate with Severity of Co-Morbid Estrous Cycle Disruption. A subset of KA-injected females can maintain regular estrous cyclicity through 2 months after injection (Li et al., 2017). This resilience may reflect inaccuracy of the initial injection or reduced induction of hippocampal damage. Therefore, the hippocampi of all KA-injected females that maintained regular 4-6 d estrous cycles (KA-regular) were examined by histology, even if acute seizures were detected in the videos. Hippocampi of 12

351 out of the 20 mice (60%) in this group showed granule cell dispersion in Cresyl Violet staining
352 (**Figure 2A**). 7 of the remaining 8 mice showed gliosis with GFAP staining (**Figure 2B**). The
353 remaining mouse was not confirmed by histology due to problems with tissue sectioning, but
354 remained in the final dataset as it was confirmed to have shown acute seizures.

355 To determine whether the presentation of sclerosis was higher in mice that developed
356 prolonged estrous cycle lengths ($\geq$7 d period, KA-long), we evaluated the hippocampi of 25
357 randomly selected KA-long mice. 19 of these mice (76%) showed sclerosis in Cresyl Violet
358 staining; this proportion was not different from that of the KA-regular group ($p>0.6$, Chi-square
359 test). These results indicate that the severity of co-morbid estrous cycle disruption following KA
360 injection is not directly correlated with the rate of induction of hippocampal sclerosis, and that
361 downstream changes in the HPG axis likely play a significant role in driving the co-morbidity.

362

363 **GnRH Neurons from KA-Injected Female Mice Show Altered Firing Rates on Diestrus and**
364 **Estrus.** For studies of female mice, acute coronal brain slices were prepared on either diestrus
365 or estrus ~2 months after intrahippocampal saline/KA injection. Targeted extracellular loose
366 patch recordings were performed to detect spontaneous action currents, the fast currents
367 underlying action potentials (**Figure 3A**), in GnRH neurons. All GnRH neurons recorded were
368 ipsilateral to the injected hippocampus. tdTomato$^+$ somata in the medial septum (MS), preoptic
369 area (POA), and anterior hypothalamic area (AHA) displaying the bipolar morphology typical of
370 GnRH neurons were targeted for recording. GnRH neurons from control mice typically showed
371 firing activity with periodic quiescence between groups (bursts) of action currents (**Figure 3B**).

Cells recorded on estrus had higher mean firing rates than cells recorded on diestrus (diestrus n=16 cells/8 mice, estrus n=20 cells/9 mice; p=0.03; Mann-Whitney test) (**Figure 3C-D**), providing novel evidence for an endogenous diestrus-to-estrus shift in mean firing rate in control conditions.

By contrast, GnRH neurons from KA-injected females showed abnormal firing patterns (**Figure 3B**). On diestrus, GnRH neurons from KA-long mice (n=17 cells/9 mice) showed an increase in mean firing rate compared with both control (n=16 cells/8 mice, p=0.01) and KA-regular mice (n=20 cells/10 mice, p=0.016; Kruskal-Wallis test/Dunn's). The mean firing rate of GnRH neurons from KA-regular females was not different from controls (**Figure 3C**). GnRH neurons from KA-long females showed high firing rates $\leq$3.8 Hz, although firing rates for some cells fell within the normal range (**Figure 3D**). When the data from KA-long and KA-regular females were combined, there was a positive linear correlation between firing rate and cycle length on diestrus (r=0.33, p=0.043, Spearman's Rank-Order test) (**Figure 3E**). These results suggest that the impacts of KA injection on GnRH neuron firing activity on diestrus are correlated with the severity of co-morbid estrous cycle disruption.

On estrus, GnRH neurons from both KA-long (n=18 cells/8 mice, p=0.01) and KA-regular (n=17 cells/7 mice, p=0.01) females showed significantly lower firing rates compared with controls (n=20 cells/9 mice) (**Figure 3C,** Kruskal-Wallis test/Dunn's). Some cells from KA-long and KA-regular females showed only a few or no action potentials (**Figure 3D**). GnRH neuron firing rate and estrous cycle length were not correlated on estrus (r=0.082, p=0.64, Spearman's test) (**Figure 3E**). Therefore, in contrast to the results obtained on diestrus, the impacts of KA injection on the firing activity of GnRH neurons on estrus are similar in mice with and without

394 co-morbid estrous cycle disruption. Moreover, the KA-induced impact on activity of GnRH
395 neurons from KA-long mice is opposite that observed on diestrus.

396 Notably, in contrast to the typical elevation in firing on estrus compared with diestrus in
397 control mice, the diestrus-to-estrus shift in firing was reversed in KA-long mice, with decreased
398 firing on estrus compared with diestrus ($p<0.0001$; Mann-Whitney test). Although mean firing
399 rates of cells from KA-regular mice were similar between diestrus (0.39 $\pm$ 0.08 Hz) and estrus
400 (0.29 $\pm$ 0.13 Hz), a nonparametric Mann-Whitney test revealed a significant difference ($p=0.03$),
401 which appeared to be driven mainly by a subset of neurons with firing rates close to zero on
402 estrus (**Figure 3D**). These results suggest that KA injection disrupts the normal patterns of
403 diestrus vs. estrus changes in GnRH neuron firing activity.

404

405 **GnRH Neuron Location Influences Firing Rate Response to KA Injection.** To determine whether
406 the firing rate phenotype of each cell was influenced by the soma location, the recorded GnRH
407 neurons were classified based on the location of the recording pipette tip in the MS, POA, or
408 AHA. Although this analysis necessitated parsing the overall data into more groups, some of
409 which only had a few cells, distinct patterns emerged based on the anatomical classification.

410 On diestrus, GnRH neurons in the MS from KA-long females (n=4 cells/4 mice) showed
411 higher firing rates than cells from controls (n=6 cells/3 mice, $p=0.034$) and KA-regular mice (n=4
412 cells/4 mice, $p=0.043$, Kruskal-Wallis test/Dunn's). GnRH neurons in the POA from KA-long
413 females (n=10 cells/7 mice) had higher firing rates than neurons from controls (n=7 cells/6 mice,
414 $p=0.025$), and a borderline level of significance in comparison to neurons from KA-regular mice

(n=11 cells/9 mice, p=0.053, Kruskal-Wallis test/Dunn's). Firing rates of cells in the AHA, however, were not different between the three groups (saline n=3 cells/3 mice, KA-long n=3 cells/3 mice, KA-regular n=5 cells/5 mice, p>0.8) (**Figure 3F**).

On estrus, GnRH neurons in the MS and POA from both KA-long (n=5 cells/4 mice MS, 8 cells/7 mice POA) and KA-regular (n=5 cells/5 mice MS, 7 cells/6 mice POA) females displayed decreased firing rates compared to controls (n=6 cells/5 mice MS, 8 cells/6 mice POA) (MS: KA-long vs. saline p=0.019, KA-regular vs. saline p=0.042; POA: KA-long vs. saline p=0.037, KA-regular vs. saline p=0.045, Kruskal-Wallis/Dunn's). Cells in the AHA from KA-long females recorded on estrus (n=5 cells/5 mice) showed decreased firing compared with controls (n=6 cells/5 mice; KA-long vs. saline p=0.027; Kruskal-Wallis test/Dunn's), but cells from KA-regular mice (n=5 cells/4 mice) were not different from controls (**Figure 3G**). Together, these results indicate that, on both diestrus and estrus, firing rates of GnRH neurons in the MS and POA are most strongly affected following KA injection. On estrus, however, AHA cells also appear to be affected in mice with the most severe co-morbid estrous cycle disruption.

GnRH Neuron Firing Patterns are Altered Following KA Injection in Female Mice. The full spike train of each recorded GnRH neuron was used to categorize firing patterns by constructing ISI joint scatter plots. The scatter plots were divided into four quadrants (clusters) by a series of candidate burst ISI threshold values. The optimal value among the candidate burst ISI thresholds was determined as the value at which the degree of proximity was highest for all four clusters, quantified as the intersection point of the cluster limit lines producing the lowest

436 squared summed distance between all points within a cluster and its respective centroid
437 (center of the cluster) (**Figure 4A**).

438 In accordance with other studies of GnRH neuron firing pattern *in vitro* and *in vivo*
439 (Moenter et al., 2003; Constantin et al., 2013), the neurons recorded in this dataset showed
440 bursting, irregular spiking, or tonic spiking patterns (**Figure 4B**). When a neuron shows a
441 bursting pattern, each quadrant (C1-C4) on the ISI scatter plot contains a cluster that
442 encompasses the spikes within bursts, at the beginning of each burst, at the end of each burst,
443 and outside the burst, respectively. In bursting neurons, the spikes in cluster C1 (lower left
444 quadrant) outnumber other clusters, producing a skewed distribution of ISI values across
445 clusters. The number of spikes to define a burst was set greater than or equal to 4. Therefore,
446 for a cell to be identified as a bursting neuron, the C1 cluster needed to contain at least 2 times
447 as many points as C2 (lower right) and C4 (upper left), and at least 5 times as many points as C3
448 (upper right) in the ISI joint scatter plot. When a neuron showed an irregular or tonic spiking
449 pattern, the ISI values were divided almost equally across the 4 quadrants. Neurons were
450 classified as tonic spiking when the centroids for all clusters were located at ISI values <1 s.

451 The results of logistic regression analysis for each firing pattern examining effects of KA
452 injection, cycle stage, and interaction between KA injection and cycle stage are summarized in
453 **Table 2**. For burst firing, there were no effects of KA injection or cycle stage, and no interaction.
454 For irregular spiking, there was an effect of cycle stage, but no effect of KA injection and no
455 interaction. For tonic spiking, there were no effects of cycle stage or KA injection separately,
456 but there was a significant interaction. For quiet cells, there were effects of both KA injection
457 and cycle stage, but no interaction.

458 Group-specific differences for irregular, tonic, and quiet activity were further analyzed
459 *post hoc* using pair-wise Fisher's exact tests (**Figure 4C**). Cells from saline-treated controls
460 showed a greater proportion of cells showing irregular spiking on diestrus compared with
461 estrus (p=0.034). Analysis of tonic spiking showed a borderline significant difference between
462 diestrus and estrus (p=.053). Cells from KA-long mice showed more tonic firing on diestrus than
463 on estrus (p=.045), and cells from KA-regular mice showed more irregular spiking on diestrus
464 than on estrus (p=.049) and more quiescence on estrus than on diestrus (p=.014).

465 On diestrus, no differences were detected between KA-injected groups and controls for
466 any firing pattern, but comparisons between the KA-long and KA-regular groups found that cells
467 from KA-regular mice showed increased irregular spiking (p=.049), with no differences detected
468 for tonic firing or quiescence. On estrus, cells from control mice showed more tonic firing in
469 comparison to both KA-long (p=.048) and KA-regular (p=.049) groups. Cells from KA-regular
470 mice also showed increased quiescence compared with controls (p=.014). No differences were
471 detected between KA-long and KA-regular groups on estrus.

472 On diestrus, the tonic-spiking neurons from KA-long females were in the POA (3 neurons)
473 and MS (1 neuron), and the one tonic-spiking neuron from a KA-regular female was in the POA.
474 On estrus, the tonic-spiking neurons from controls were in the AHA (3 neurons), POA (1 neuron),
475 and MS (1 neuron), and quiet cells from both KA-long and KA-regular females were in the POA
476 and MS (KA-long: 2 POA, 1 MS; KA-regular 3 POA, 2 MS). Bursting and irregular-spiking cells in
477 all groups were evenly distributed across the MS, POA, and AHA. These results indicate that
478 following KA injection, a subset of GnRH neurons in the MS and POA displays a continuous tonic
479 firing activity pattern on diestrus that is not observed in controls. Furthermore, in stark contrast

to the firing patterns observed on diestrus, subsets of GnRH neurons in the MS and POA show aberrant quiescence on estrus after KA injection.

GnRH Neuron Burst Properties are Altered Following KA Injection in Female Mice. To assess whether GnRH neuron burst firing (which may be linked to hormone release) is altered after KA injection, the cells that were categorized as "bursting" were further examined for detailed analysis of burst properties. Note that because bursting cells were distributed across all 3 anatomical areas examined, location categories were collapsed for this analysis.

GnRH neurons from control mice showed distinct burst properties between diestrus and estrus. Bursting cells showed longer burst duration, more spikes per burst, and slower intraburst firing rate on estrus compared with diestrus (diestrus n=8 cells, estrus n=12 cells; all $p<0.0001$, pairwise Kolmogorov–Smirnov tests). The intervals between bursts were also longer on estrus than on diestrus ($p<0.0001$) (**Figure 5A**). GnRH neurons from KA-long females did not display the difference in burst duration and number of spikes per burst between cycle stages, but intraburst firing rate was decreased and interburst interval was longer on estrus than on diestrus (diestrus n=10 cells, estrus n=10 cells; both $p<0.0001$, pairwise Kolmogorov–Smirnov tests) (**Figure 5B**). GnRH neurons from KA-regular females showed the same directions of change as controls (diestrus n=6 cells, estrus n=5 cells), with increased burst duration, number of spikes per burst, and interburst interval, as well as decreased intraburst firing rate, on estrus compared with diestrus (all $p<0.0001$, pairwise Kolmogorov–Smirnov tests) (**Figure 5C**). These results demonstrate that GnRH neuron burst properties fluctuate with the estrous cycle,

showing changes indicative of increased bursting (and potentially increased hormone release) on estrus compared with diestrus.

On diestrus, cells from KA-injected mice showed increased burst duration and number of spikes per burst compared with controls (saline n=8 cells; KA-long n=8 cells; KA-regular n=6 cells; pairwise Kolmogorov–Smirnov tests: KA-long vs. saline: $p<0.0001$, KA-regular vs. saline: $p<0.0001$) (**Figure 6A**). The distributions of values for KA-long and KA-regular groups, however, were also distinct from each other, with the KA-long group showing increased probability of the longest burst durations and highest numbers of spikes per burst ($p<0.0001$). In comparison to controls, cells from KA-long females showed higher intraburst firing rates ($p<0.0001$), but conversely, cells from KA-regular females showed decreased intraburst firing rates ($p<0.0001$). In addition, the intervals between bursts were prolonged in GnRH neurons from KA-regular females compared with controls ($p=0.0006$) (**Figure 6A**), but cells from KA-long females did not show this difference. These latter findings of decreased intraburst firing rate and increased interburst interval in cells from KA-regular mice may represent compensatory mechanisms engaged to decrease burst-driven GnRH release in this group.

On estrus, GnRH neurons from KA-long females displayed shorter bursts, fewer spikes per burst, and higher intraburst firing rates than controls (saline n=12 cells; KA-long n=10 cells; all $p<0.0001$, pairwise Kolmogorov–Smirnov tests). GnRH neurons from KA-regular females (n=5 cells), however, showed changes in the opposite direction, with longer burst duration, more spikes per burst, and slower intraburst firing rate than controls (all $p<0.0001$). GnRH neurons from KA-regular females also showed an altered distribution of interburst interval values compared to those from KA-long females and controls ($p<0.0001$) (**Figure 6B**). These findings

indicate that, although overall firing rates between cells from KA-long and KA-regular females are similar on estrus, the burst properties are quite different. Moreover, the burst properties of cells from KA-regular mice on estrus show the same pattern of differences compared with controls as observed on diestrus. For cells from KA-long mice, however, the effects on burst duration and number of spikes per burst on estrus in comparison to controls are opposite those observed on diestrus.

GnRH Neuron Intrinsic Excitability Changes from Diestrus to Estrus and is Persistently Increased in KA-Injected Female Mice. We used whole-cell current-clamp recordings to determine whether the observed changes in firing activity are associated with changes in intrinsic excitability. Three-way ANOVA showed treatment group, estrous cycle stage, and soma location all had effects on the GnRH neuron evoked firing rate (treatment group and estrous cycle: $p<0.001$, soma location $p=0.019$). Neurons in the control group had higher evoked firing rates on estrus than on diestrus (diestrus = 18 cells/8 mice, estrus = 20 cells/5 mice, $p=0.005$, three-way ANOVA/Fisher's LSD) (**Figure 7A-C**), indicating an endogenous increase in excitability on estrus compared with diestrus in control conditions.

Because there was no interaction between treatment group and estrous cycle stage ($p=0.13$, overall three-way ANOVA), the data from diestrus and estrus were initially combined to examine the overall effects of KA injection on GnRH neuron excitability. In this analysis, GnRH neurons from both KA-long and KA-regular females showed increased excitability compared with controls (saline n=38 cells/13 mice, KA-long n=41 cells/13 mice, KA-regular n=30

cells/11 mice; saline vs KA-long, $p<0.001$, saline vs KA-regular, $p=0.001$) (**Figure 7B-C**). Furthermore, comparisons made examining each cycle stage separately identified elevated excitability in both KA-injected groups compared with controls on both diestrus and estrus ([diestrus: saline n=18 cells/8 mice, KA-long n=26 cells/8 mice, KA-regular n=15 cells/7 mice; saline vs. KA-long $p=0.047$, saline vs. KA-regular $p=0.008$, Fisher's LSD] [estrus: saline n=20 cells/5 mice, KA-long n=15 cells/5 mice, KA-regular n=15 cells/4 mice; saline vs. KA-long $p<0.001$, saline vs. KA-regular $p=0.045$, Fisher's LSD]). These results suggest that GnRH neuron intrinsic excitability is elevated in mice both with and without co-morbid estrous cycle disruption after KA injection, and that this higher excitability persists across both diestrus and estrus.

Fisher's LSD *post hoc* tests were used to examine the differences between control and KA-injected groups with respect to soma location. Specifically, GnRH neurons from KA-long females in MS and POA, but not in AHA, showed increased excitability compared with controls at both cycle stages (MS $p=0.048$ diestrus, $p<0.001$ estrus; POA $p=0.021$ diestrus, $p=0.027$ estrus; n=5-13 cells for each group and location). Only GnRH neurons in MS from KA-regular females showed increased excitability compared with controls at both cycle stages (diestrus $p = 0.003$, estrus $p = 0.027$; n=5-9 cells for each location). No difference was observed between KA-long and KA-regular groups in either MS or POA, and no effect of KA injection was observed in the AHA region (**Figure 7B**). These results suggest that, as with the effects on overall firing rate, GnRH neurons in the MS and POA show the greatest change in excitability after KA injection.

To investigate whether KA-injected females also showed cycle stage-dependent fluctuations in GnRH neuron excitability as observed in the control mice, evoked firing rates from KA-injected mice were compared between diestrus and estrus. Cells from KA-long females

showed higher excitability on estrus compared with diestrus ($p<0.001$). Cells from KA-regular females showed a similar trend but not to the level of significance ($p=0.067$) (**Figure 7C**). Together with the changes in burst firing specific to the KA-regular group described above, this trend may also represent a compensatory mechanism to bring intrinsic excitability values closer to the control range, particularly on estrus.

Additional excitability parameters were analyzed to evaluate potential mechanisms of increased GnRH neuron evoked firing rate observed in cells from KA-injected female mice. These parameters included action potential (AP) threshold, input resistance, capacitance, membrane time constant (Tau), latency to firing, interspike interval, and instantaneous frequency. Because cells in the MS and POA, but not AHA, showed changes in evoked firing rate, these excitability parameters were analyzed for MS and POA cells only. Three-way ANOVA showed that the soma location did not affect any of the tested parameters. Therefore, the data from both MS and POA were grouped together for further analysis. On diestrus, neurons from KA-long and KA-regular females showed hyperpolarized AP threshold compared with controls ($p=0.021$ KA-long vs. saline, $p<0.001$ KA-regular vs. saline, two-way ANOVA/Fisher's LSD). On estrus, neurons from KA-long, but not KA-regular, females showed hyperpolarized AP threshold ($p=0.038$, two-way ANOVA/Fisher's LSD) and increased Tau ($p=0.006$, two-way ANOVA/Fisher's LSD) compared with controls (**Figure 7D**). No differences were seen in input resistance or the other parameters (**Figure 7D, Table 3**). None of the action potential kinetics parameters examined (full-width at half-maximum, afterhyperpolarization amplitude, time to afterhyperpolarization, rise slope and decay slope) were different between control and KA-injected groups (**Table 3**). Together, these results indicate that the observed changes in overall

588 intrinsic excitability are manifest most notably in hyperpolarized AP threshold on both diestrus
589 and estrus, and increased membrane time constant on estrus. Furthermore, these effects are
590 most prominent in GnRH neurons from KA-injected mice with more severe estrous cycle
591 disruption.

592 Comparisons of GnRH neuron excitability parameters within groups between diestrus
593 and estrus also indicated differences. AP threshold was hyperpolarized on estrus compared
594 with diestrus in control mice ($p=0.022$), but not in KA-long or KA-regular mice (KA-long $p=0.063$,
595 KA-regular $p=0.9$). Tau was increased on estrus compared with diestrus in control and KA-long
596 mice (saline $p=0.013$, KA-long $p<0.001$), but not in KA-regular mice ($p=0.12$) (**Figure 7D**). These
597 results indicate that KA-injected groups do not display the typical diestrus-to-estrus difference
598 in AP threshold observed in controls. In addition, a lack of diestrus vs. estrus difference in
599 membrane time constant may represent another compensatory mechanism specific to the KA-
600 regular group.

601

602 **Changes in Circulating P_4 and E_2 Levels Two Months After KA Injection in Females.** Changes in
603 GnRH neuron activity could impact downstream gonadal function, including production and
604 secretion of sex steroids. Reciprocally, sex steroid feedback can act at the hypothalamic level to
605 affect GnRH neuron activity, and at the hippocampal level to modulate seizure susceptibility.
606 Therefore, to determine whether circulating levels of the female sex steroid hormones P_4 and
607 E_2 are altered in the intrahippocampal KA mouse model of TLE, we assayed trunk blood serum
608 by ELISA. In controls, P_4 levels were higher on estrus than on diestrus (diestrus=23 mice,

609 estrus=18 mice, p=0.01, two-sample t-test). In KA-long and KA-regular mice, P_4 levels were not
610 significantly different between diestrus and estrus (KA-long diestrus n=19 mice, estrus n=10
611 mice, p>0.6; KA-regular diestrus n=20 mice, estrus n=7 mice, p=0.14). Serum P_4 levels were
612 reduced in KA-long females compared with both controls and KA-regular females on both
613 diestrus (KA-long vs. saline p=0.042, KA-long vs. KA-regular p=0.02; one-way ANOVA/Fisher's
614 LSD) and estrus (KA-long vs. saline p=0.036, KA-long vs. KA-regular p=0.007; one-way
615 ANOVA/Fisher's LSD). P_4 levels in KA-regular females were not different from controls at either
616 cycle stage (p>0.3) (**Figure 8A**). These results indicate that suppression of P_4 levels on both
617 diestrus and estrus is associated with increased severity of co-morbid estrous cycle disruption
618 after KA injection.

619 In control mice, serum E_2 levels were lower on estrus than diestrus (diestrus=6 mice,
620 estrus=6 mice, p=0.035, two-sample t-test). In KA-long and KA-regular mice, the E_2 levels were
621 not significantly different between diestrus and estrus (KA-long diestrus n=8 mice, estrus n=10
622 mice p=0.59; KA-regular diestrus n=6 mice, estrus n=5 mice p=0.07). On diestrus, E_2 levels were
623 not different between the three groups, but on estrus E_2 levels were significantly higher in KA-
624 injected females compared with controls (KA-long vs. saline p=0.036, KA-regular vs. saline
625 p=0.016; one-way ANOVA/Fisher's LSD), with no difference observed between KA-long and KA-
626 regular females (**Figure 8B**). These results indicate that KA-injected mice both with and without
627 co-morbid estrous cycle disruption lack the typical decrease in E_2 levels on estrus compared
628 with diestrus.

629

Male Mice Show Modest Disruption of GnRH Neuron Activity After KA Treatment Without Changes in T Levels. An advantage of integrating mouse models of TLE with GnRH-tdTomato mice is that we can also assess impacts of epilepsy on GnRH neurons from male mice, which lack a parameter akin to the estrous cycle that can be used as a high-throughput assay of reproductive endocrine co-morbidities. To determine whether the effects of KA treatment on GnRH neurons are sex-specific, we measured firing rate, burst properties, and intrinsic excitability of GnRH neurons from control and KA-injected male mice at 2 months after surgery. There was not a change in overall mean firing rate between KA-injected and control groups (saline n=18 cells/10 mice, KA n=25 cells/13 mice, p=0.14) (**Figure 9A**), but comparison of mean firing rates based on soma location revealed that MS GnRH neurons from KA-injected males displayed increased firing compared with controls (saline n=5 cells, KA n=7 cells, p = 0.034, Mann-Whitney test) (**Figure 9B**). Burst properties were altered, with longer burst duration and increased number of spikes per burst observed in the KA-injected group (saline n=5 cells, KA n=6 cells, both $p<0.0001$, pairwise Kolmogorov–Smirnov tests) (**Figure 9C**). The saline-injected mice had bursting GnRH neurons in the POA (4 neurons) and AHA (1 neuron), whereas the KA-injected mice had bursting GnRH neurons in the POA (5 neurons) and MS (1 neuron). The intraburst firing rate and interburst interval were not different between control and KA-injected groups (**Figure 9C**), and the proportion of GnRH neurons from male mice showing irregular spiking or bursting was not affected by KA treatment (control: 61% irregular and 39% bursting; KA-injected: 72% irregular and 28% bursting; $p>0.5$, Chi-square test). No cells showed tonic spiking or quiet patterns. These results suggest that the impacts of KA injection on GnRH neuron firing are different in males compared with females.

In whole-cell current-clamp recordings, GnRH neurons in the MS and POA from KA-injected males showed higher evoked firing rates compared with controls (MS p=0.028, POA p=0.044, two-way ANOVA/ Fisher's LSD; n=5-10 cells for each group and location) (**Figure 9D**). Cells in the AHA did not show a KA-induced difference in excitability. No other parameters of excitability and action potential kinetics were different between control and KA-injected males (**Table 4**). These results indicate that, as observed in females, excitability of MS and POA GnRH neurons is elevated in KA-injected males, although the change in excitability is limited to evoked firing rate. In addition, serum T levels in KA-injected males were not different from controls (**Figure 9E**).

Discussion

Pathologies in the neural control of reproduction likely link epilepsy and co-morbid reproductive endocrine disorders, but specific functional changes in key neuronal populations regulating reproduction and fertility, including GnRH neurons, have not been described. The present studies provide direct evidence for changes in GnRH neuron function with epilepsy, and indicate that impacts on GnRH neuron function are associated with severity of co-morbid estrous cycle disruption, different on diestrus compared with estrus, and sex-specific. Overall, GnRH neurons from KA-injected diestrous females, estrous females, and males shared some commonalities as well as some group-specific changes. GnRH neurons in the MS and POA showed increased evoked firing rates across all groups, but only females showed significantly hyperpolarized AP threshold. In addition, these results are the first to show that unilateral KA

injection alters circulating sex hormone levels in female mice. Due to the complex feedback loops involved, at present it remains difficult to distinguish changes that are direct consequences of epileptiform activity in the hippocampus from those that are secondary alterations that develop as a feedback response to co-morbid estrous cycle disruption. The changes common to all groups, however, likely reflect the direct consequences of KA-induced epilepsy.

Linking hippocampal seizure activity to changes in hypothalamic GnRH neuron function

Seizures in TLE originate primarily in the hippocampus and rarely become generalized (Engel, 1996). The intrahippocampal KA mouse model of TLE similarly shows recurrent spontaneous paroxysmal discharges mainly restricted to the vicinity of the injected hippocampal area (Riban et al., 2002), although recent work using cortical surface recordings in the same model detected generalized spikes propagating across frontal cortices as well (Sheybani et al., 2018). Whether there is a correlation between hippocampal seizure burden and temporal proximity of recent seizure activity to GnRH neuron functional abnormalities and estrous cycle disruption will be investigated by incorporating electroencephalogram recordings in future studies. In this regard, spontaneous seizures in the intrahippocampal KA mouse model are present by approximately 2 weeks after KA injection (Riban et al., 2002; Heinrich et al., 2011), whereas the estrous cycle disruption in this model does not emerge until approximately 6 weeks after KA injection (Li et al., 2017). This time course indicates that the robust pattern of disrupted estrous cyclicity develops gradually after epilepsy is fully established, perhaps

694 reflecting a cumulative effect of seizure burden over time (Raedt et al., 2009). This temporal
695 sequence should provide important insights in future studies about the causal relationships
696 between epileptogenesis, seizure severity, GnRH neuron pathology, and estrous cycle
697 disruption.

698 Focal hippocampal seizures could potentially affect GnRH neurons through direct and/or
699 indirect projections between the hippocampus and the hypothalamus. Indeed, it has long been
700 known that electrical stimulation in hippocampus can reduce gonadotropin release and prevent
701 ovulation, indicating functional links between the hippocampus and hypothalamic circuits for
702 reproduction (Velasco and Taleisnik, 1969; Gallo et al., 1971). The present data indicate that
703 GnRH neurons with aberrant firing activity in females are primarily located in the MS and POA.
704 Similarly, the MS is the only region that contained GnRH neurons with increased firing rates in
705 male mice, although cells in the POA showed altered bursting properties. There are robust
706 bidirectional projections between the hippocampus and the MS (Gaykema et al., 1991; Mattis
707 et al., 2014). The prominence of KA-induced changes in GnRH neurons located in the MS
708 suggests that these pathways may provide anatomical substrates for seizure activity and/or the
709 secondary consequences of hippocampal epileptiform activity to propagate and impact
710 hypothalamic GnRH neurons. The extent and characteristics of reorganization of hippocampal
711 projections to GnRH neuron circuitry following intrahippocampal KA injection remain unclear.
712 Furthermore, GnRH neurons form a heterogeneous population with variations, for example, in
713 firing properties (Constantin et al., 2013), neuromodulator receptor expression (Jasoni et al.,
714 2005), and participation in the preovulatory GnRH/LH surge (Hoffman et al., 1993;
715 Wintermantel et al., 2006; Christian and Moenter, 2007) associated with differences in soma

location. The relationship between the anatomical location of GnRH neuron somata and cellular heterogeneity has not yet been fully characterized, but the present data support a working model in which the location of the GnRH neuron soma helps to shape the functional outcome in the face of epilepsy, in concert with changes in hippocampal-hypothalamic projections differentially targeting the MS, POA, and AHA.

Pathologic hallmarks of TLE in hippocampus and hypothalamus

Hippocampal sclerosis is a common hallmark of TLE in humans (Margerison and Corsellis, 1966; Cook et al., 1992; Blümcke et al., 2013; Blumcke et al., 2017). The intrahippocampal KA mouse model of TLE reproduces this hippocampal sclerosis in multiple ways, including extensive neuronal loss, gliosis, and hippocampal circuit reorganization. Specifically, the complete degeneration of CA1 and CA3 is often observed in ipsilateral dorsal hippocampus, along with enlargement of the dentate granule cell layer (Bouilleret et al., 1999; Riban et al., 2002) (**Figure 2A**). Although intrahippocampal KA injection induces acute injury and cell loss, it should be noted that estrous cyclicity can persist following complete ablation of the hippocampus in rats (Terasawa and Kawakami, 1973). Furthermore, we observed similar rates of hippocampal sclerosis induction in both KA-long and KA-regular groups. Therefore, the changes observed in GnRH neuron function likely reflect epileptic circuit reorganization and downstream propagating effects of seizure activity, rather than acute effects of the initial precipitating hippocampal injury *per se* (i.e., effects independent of epileptiform activity). The extent of hypothalamic pathology in the intrahippocampal KA mouse model used here remains

737 unclear. However, neither cell loss nor gliosis were observed in the hypothalamus in a unilateral
738 KA macaque model of epilepsy (Chen et al., 2013), and no GnRH neuron cell loss was observed
739 in a systemic pilocarpine mouse model (Fawley et al., 2012).

740

741 *Changes in GnRH neuron firing properties: potential links to downstream HPG axis malfunction*

742 Changes in LH pulse frequency have been reported in women with epilepsy in the
743 absence of antiepileptic drug treatment, even when regular menstrual cyclicity is maintained
744 (Bilo et al., 1991; Meo et al., 1993). Altered GnRH-LH release in patients with epilepsy may thus
745 represent a form of subclinical reproductive dysfunction. Because hormone secretion by
746 neuroendocrine cells, such as vasopressin and oxytocin neurons, has long been linked with
747 burst firing activities (Wakerley and Lincoln, 1973; Dutton and Dyball, 1979), we examined
748 whether KA injection affected GnRH neuron firing patterns and/or burst properties. Although
749 the proportions of cells showing burst firing were not altered following KA injection, there were
750 significant differences in burst properties in cells from both KA-injected male and female mice.
751 Moreover, the changes observed in KA-injected female mice were distinct depending on
752 whether estrous cycles were of regular or long length, indicating that changes in GnRH neuron
753 burst patterning differ with the severity of the co-morbidity. High and low GnRH pulse
754 frequency favors the pituitary synthesis and release of LH and follicle-stimulating hormone,
755 respectively (Wildt et al., 1981), but the effect of GnRH pulse duration (perhaps reflected in
756 burst duration) on gonadotropin release is still unknown. In addition, the aberrant presence of
757 tonic spiking neurons on diestrus and quiet neurons on estrus could potentially impair overall

758 GnRH neuron network communication and rhythmicity. In this regard, GnRH neurons express
759 GnRH receptors and the firing activity of GnRH neurons changes in response to application of
760 GnRH (Xu et al., 2004; Todman et al., 2005; Han et al., 2010). At the pituitary level, higher rates
761 of GnRH neuron firing activity may also give rise to sustained elevations in GnRH content in the
762 pituitary vasculature, which could downregulate the pituitary response to GnRH (Belchetz et al.,
763 1978; Smith et al., 1983). Further studies are thus needed to determine whether altered GnRH
764 neuron firing patterns drive dysregulated GnRH and gonadotropin secretion in epilepsy.

765 On diestrus, there was a moderate but significant correlation between GnRH neuron
766 firing rate and estrous cycle length in KA-injected mice, indicating a relationship between
767 elevated GnRH neuron activity and the severity of the estrous cycle co-morbidity. The estrous
768 cycle is regulated by a complex interplay involving hypothalamic GnRH release, pituitary
769 gonadotropin release, and ovarian response. Although it is unknown whether LH or FSH release
770 is altered in this model of epilepsy, the ovaries do not show major histopathological changes at
771 2 months after KA injection (Li et al., 2017), indicating that the estrous cycle phenotype is not
772 reflective of gross ovarian damage. Therefore, although it would be premature to directly link
773 the changes in GnRH neuron mean firing rate to the effects on estrous cyclicity, the positive
774 correlation observed indicates that changes in GnRH neuron activity, and potentially
775 downstream pituitary gonadotropin release, are likely to be major players in this co-morbidity.

776

777 *Relationships of sex steroid feedback and epilepsy-associated changes in GnRH neuron activity*

778 Changes in GnRH neuron firing could be, at least in part, the consequences of altered
779 sex hormone feedback. P_4 typically exerts strong suppression of GnRH neuron activity (Pielecka

et al., 2006; Bashour and Wray, 2012) and GnRH release (Goodman and Karsch, 1980; Leipheimer et al., 1984; He et al., 2017). Our finding of decreased P_4 levels (and the likely reduction of P_4 negative feedback) in KA-long females on diestrus is thus consistent with the increased mean firing rate observed in this group. P_4 levels were also reduced in KA-long females on estrus, but this change is not consistent with the significantly suppressed firing rate of GnRH neurons from this group at this stage, suggesting other mechanisms are likely involved. P_4 may still play a role in driving suppressed firing in KA-regular females on estrus, however, as this group did not show a reduction in circulating P_4.

On both diestrus and estrus, E_2 levels were within the low physiological range in which E_2 typically exerts negative (i.e., suppressive) feedback on GnRH release (Sarkar and Fink, 1980; Evans et al., 1994). Control mice had higher E_2 levels on diestrus compared to estrus. This result is in line with the lower GnRH neuron firing rate on diestrus, although an alternative possibility is that the boost in GnRH neuron firing rate observed on early estrus reflects the tail end of the robust increase in firing activity that drives the preovulatory GnRH surge during late proestrus (Christian and Moenter, 2010). Furthermore, the increased E_2 levels on estrus in both KA-long and KA-regular females would be predicted to exert increased negative feedback on GnRH neurons, and are thus consistent with the decreased GnRH neuron firing rate observed at this cycle stage in both groups. Serum E_2 levels on diestrus were similar between KA-injected and control females, suggesting that E_2 does not contribute to the observed increase in GnRH neuron firing on diestrus in the KA-long group. These differences in circulating P_4 and E_2 levels could reflect altered ovarian steroidogenesis and/or compromised metabolism of sex steroids by peripheral cytochrome P450 oxidases (Runtz et al., 2018). Mechanistic investigation of the

802 roles of E_2 and P_4 feedback in mediating epilepsy-associated changes in GnRH neuron function
803 will be an important aspect of future study, for example through selective hormone
804 replacement in gonadectomized mice, or incorporation of mouse models in which specific
805 steroid hormone receptors are absent or not functional.

806 Alterations in circulating steroid levels could also exert impacts at the level of
807 hippocampus to modulate seizure activity. For example, central P_4 conversion to the
808 neurosteroid allopregnanolone can reduce seizure susceptibility and epileptiform activity
809 through potent positive allosteric modulation of hippocampal $GABA_A$ receptors (Maguire et al.,
810 2005; Lawrence et al., 2010; Reddy and Rogawski, 2012). Therefore, reduced P_4 levels in the KA-
811 long mice may also be indicative of reduced neurosteroid production in the brain, which could
812 exacerbate seizure activity in this group.

813 In a previous study examining the systemic pilocarpine model of TLE in female rats,
814 circulating T was elevated concomitant with the presence of cystic ovaries (Scharfman et al.,
815 2008). In the present studies, measurement of T in the females was inconclusive because the
816 serum amounts that remained after completing the assays for P_4 and E_2 were too small to be
817 reliably assayed in duplicate. However, it should be noted that many values were below the
818 ELISA detection limit, and those samples that did yield values were not different between
819 control and KA-injected mice (unpublished observations). Together, these results suggest that
820 circulating T was not elevated in the KA-injected female mice. This finding is consistent with
821 previous work in which ovarian cysts were not observed in this mouse model of TLE (Li et al.,
822 2017), and thus elevated T levels would not be expected.

Of note, the pattern of changes in E_2 and P_4 levels detected in this mouse model does not directly match changes in sex steroid levels reported in a limited number of human clinical studies (Herzog et al., 2003; Kalinin and Zheleznova, 2007). Human TLE, however, is a more heterogeneous condition than one animal model can reproduce. The location of seizure origin, the effects of different anti-epileptic drugs, and timing of hormone level measurement in relation to menstrual cycle stage could all profoundly influence the phenotype of changes in sex steroid levels induced by epilepsy. Further exploration of neuroendocrine disruption in both the clinic and in preclinical models is needed to elucidate the spectrum of changes that can be induced by epilepsy and seizure activity, and to determine differential mechanisms that may drive these varying outcomes.

Relative contributions of GnRH neuron intrinsic excitability and synaptic inputs in driving epilepsy-associated changes in GnRH neuron activity

In contrast to the bidirectional changes in GnRH neuron firing rate observed in KA-injected female mice, intrinsic excitability was persistently elevated in KA-injected groups on both diestrus and estrus, and irrespective of estrous cycle period phenotype. Hyperpolarized action potential threshold was the most prominent change observed in cells from KA-injected females. Tetrodotoxin-sensitive voltage-gated sodium channels control the action potential depolarization in GnRH neurons (Norberg et al., 2013), and therefore may play important roles in determining action potential threshold. GnRH neuron action potential threshold and latency to firing can also be modulated by E_2 feedback, for example through A-type potassium currents

844 (DeFazio and Moenter, 2002). Changes in these and other underlying conductances likely shape
845 the overall shifts in excitability produced both across estrous cycle stages and in response to
846 epilepsy. In addition, the persistent increase in excitability of GnRH neurons from KA-injected
847 mice, together with the dynamic changes in mean firing rate, indicate that afferent synaptic
848 and/or neuromodulatory inputs likely play a role in shaping the cycle-stage-dependent shifts in
849 overall firing behavior. In this regard, most E_2 and P_4 feedback to GnRH neurons is mediated
850 trans-synaptically (Sullivan and Moenter, 2005; Wintermantel et al., 2006; Christian and
851 Moenter, 2007), and certainly at least one synaptic connection is needed to transmit the effects
852 of hippocampal seizure activity to hypothalamic GnRH neurons. It will be interesting in future
853 studies to determine which steroid hormone-sensitive and –insensitive pathways are involved
854 in transmitting the effects of seizure activity to GnRH neurons, and in driving differential
855 changes dependent on estrous cycle stage.

856

857 *Concluding remarks*

858 The present results provide novel direct evidence of aberrant GnRH neuron activity and
859 excitability in an animal model of epilepsy. Most importantly, this study supports a model in
860 which the pattern of changes in GnRH neuron firing activity in epilepsy is not a fixed property,
861 but is profoundly influenced by the overall physiological state. Furthermore, these studies
862 emphasize the utility of this model of TLE in distinguishing which changes are observed
863 concomitant with estrous cycle disruption, and which changes are observed in resilient females
864 that maintain regular estrous cyclicity. These findings thus have important implications for

865 further studies of the neural mechanisms linking epilepsy to co-morbid reproductive endocrine
866 dysfunction, and provide an indication that treatment strategies for both seizures and
867 reproductive co-morbidities need to be tailored based on cycle stage, co-morbidity severity,
868 and sex.

869

870

871 **References**

872 Amado D, Cavalheiro E (1998) Hormonal and gestational parameters in female rats submitted
873 to the pilocarpine model of epilepsy. Epilepsy Res 32:266-274.

874 Amado D, Cavalheiro E, Bentivoglio M (1993) Epilepsy and hormonal regulation: the patterns of
875 GnRH and galanin immunoreactivity in the hypothalamus of epileptic female rats.
876 Epilepsy Res 14:149-159.

877 Amado D, Verreschi IT, Berzaghi MP, Cavalheiro EA (1987) Effects of intrahippocampal injection
878 of kainic acid on estrous cycle in rats. Braz J Med Biol Res 20:829-832.

879 Bashour NM, Wray S (2012) Progesterone directly and rapidly inhibits GnRH neuronal activity
880 via progesterone receptor membrane component 1. Endocrinology 153:4457-4469.

881 Bauer J, Cooper-Mahkorn D (2008) Reproductive dysfunction in women with epilepsy:
882 menstrual cycle abnormalities, fertility, and polycystic ovary syndrome. Int Rev
883 Neurobiol 83:135-155.

884 Bauer J, Jarre A, Klingmüller D, Elger CE (2000) Polycystic ovary syndrome in patients with focal
885 epilepsy: a study in 93 women. Epilepsy Res 41:163-167.

886 Belchetz PE, Plant TM, Nakai Y, Keogh EJ, Knobil E (1978) Hypophysial responses to continuous
887 and intermittent delivery of hypopthalamic gonadotropin-releasing hormone. Science
888 202:631-633.

889 Bilo L, Meo R, Valentino R, Buscaino GA, Striano S, Nappi C (1991) Abnormal pattern of
890 luteinizing hormone pulsatility in women with epilepsy. Fertil Steril 55:705-711.

891 Bilo L, Meo R, Valentino R, Di Carlo C, Striano S, Nappi C (2001) Characterization of reproductive
892 endocrine disorders in women with epilepsy. J Clin Endocrinol Metab 86:2950-2956.
893 Blumcke I et al. (2017) Histopathological Findings in Brain Tissue Obtained during Epilepsy
894 Surgery. N Engl J Med 377:1648-1656.
895 Blümcke I, Thom M, Aronica E, Armstrong DD, Bartolomei F, Bernasconi A, Bernasconi N, Bien
896 CG, Cendes F, Coras R (2013) International consensus classification of hippocampal
897 sclerosis in temporal lobe epilepsy: a Task Force report from the ILAE Commission on
898 Diagnostic Methods. Epilepsia 54:1315-1329.
899 Bouilleret V, Ridoux V, Depaulis A, Marescaux C, Nehlig A, La Salle GLG (1999) Recurrent
900 seizures and hippocampal sclerosis following intrahippocampal kainate injection in adult
901 mice: electroencephalography, histopathology and synaptic reorganization similar to
902 mesial temporal lobe epilepsy. Neuroscience 89:717-729.
903 Byers SL, Wiles MV, Dunn SL, Taft RA (2012) Mouse estrous cycle identification tool and images.
904 PLoS one 7:e35538.
905 Chen N, Liu C, Yan N, Hu W, Zhang J-g, Ge Y, Meng F-g (2013) A macaque model of mesial
906 temporal lobe epilepsy induced by unilateral intrahippocampal injection of kainic acid.
907 PLoS one 8:e72336.
908 Christian CA (2017) Neurophysiology of Gonadotropin-Releasing Hormone Neurons. In:
909 Hormones, Brain and Behavior, 3rd Edition (Pfaff DW, Joëls M, eds), pp 379-400
910 Academic Press: Oxford.

911 Christian CA, Moenter SM (2007) Estradiol induces diurnal shifts in GABA transmission to
912 gonadotropin-releasing hormone neurons to provide a neural signal for ovulation. J
913 Neurosci 27:1913-1921.
914 Christian CA, Moenter SM (2010) The neurobiology of preovulatory and estradiol-induced
915 gonadotropin-releasing hormone surges. Endocr Rev 31:544-577.
916 Christian CA, Mobley JL, Moenter SM (2005) Diurnal and estradiol-dependent changes in
917 gonadotropin-releasing hormone neuron firing activity. Proc Natl Acad Sci USA
918 102:15682-15687.
919 Constantin S, Iremonger KJ, Herbison AE (2013) In vivo recordings of GnRH neuron firing reveal
920 heterogeneity and dependence upon GABAA receptor signaling. J Neurosci 33:9394-
921 9401.
922 Cook MJ, Fish DR, Shorvon SD, Straughan K, Stevens JM (1992) Hippocampal volumetric and
923 morphometric studies in frontal and temporal lobe epilepsy. Brain 115 (Pt 4):1001-1015.
924 DeFazio RA, Moenter SM (2002) Estradiol feedback alters potassium currents and firing
925 properties of gonadotropin-releasing hormone neurons. Mol Endocrinol 16:2255-2265.
926 Dodla R, Wilson CJ (2010) Quantification of clustering in joint interspike interval scattergrams of
927 spike trains. Biophys J 98:2535-2543.
928 Drislane F, Coleman A, Schomer D, Ives J, Levesque L, Seibel M, Herzog A (1994) Altered
929 pulsatile secretion of luteinizing hormone in women with epilepsy. Neurology 44:306-
930 306.
931 Dutton A, Dyball RE (1979) Phasic firing enhances vasopressin release from the rat
932 neurohypophysis. J Physiol 290:433-440.

933 Edwards H, MacLusky N, Burnham W (2000) The effect of seizures and kindling on reproductive
934 hormones in the rat. Neurosci Biobehav Rev 24:753-762.
935 Edwards HE, Burnham WM, Ng MM, Asa S, MacLusky NJ (1999) Limbic seizures alter
936 reproductive function in the female rat. Epilepsia 40:1370-1377.
937 Engel J (1996) Introduction to temporal lobe epilepsy. Epilepsy Res 26:141-150.
938 Engel J, Jr. (2001) Mesial temporal lobe epilepsy: what have we learned? Neuroscientist 7:340-
939 352.
940 Evans NP, Dahl GE, Glover BH, Karsch FJ (1994) Central regulation of pulsatile gonadotropin-
941 releasing hormone (GnRH) secretion by estradiol during the period leading up to the
942 preovulatory GnRH surge in the ewe. Endocrinology 134:1806-1811.
943 Fawley J, Pouliot W, Dudek FE (2012) Pilocarpine-induced status epilepticus and subsequent
944 spontaneous seizures: lack of effect on the number of gonadotropin-releasing hormone-
945 positive neurons in a mouse model of temporal lobe epilepsy. Neuroscience 203:153-
946 159.
947 Finn DA, Gee KW (1994) The estrus cycle, sensitivity to convulsants and the anticonvulsant
948 effect of a neuroactive steroid. J Pharmacol Exp Ther 271:164-170.
949 Fox JG, Barthold S, Davisson M, Newcomer CE, Quimby FW, Smith A (2006) The Mouse in
950 Biomedical Research: Normative biology, husbandry, and models: San Diego: Academic
951 Press.
952 Friedman M, Geula C, Holmes G, Herzog A (2002) GnRH-immunoreactive fiber changes with
953 unilateral amygdala-kindled seizures. Epilepsy Res 52:73-77.

954 Gallo R, Johnson J, Goldman B, Whitmoyer D, Sawyer C (1971) Effects of electrochemical
955 stimulation of the ventral hippocampus on hypothalamic electrical activity and pituitary
956 gonadotropin secretion in female rats. Endocrinology 89:704-713.
957 Gaykema R, Van der Kuil J, Hersh L, Luiten P (1991) Patterns of direct projections from the
958 hippocampus to the medial septum-diagonal band complex: anterograde tracing with
959 Phaseolus vulgaris leucoagglutinin combined with immunohistochemistry of choline
960 acetyltransferase. Neuroscience 43:349-360.
961 Goodman RL, Karsch FJ (1980) Pulsatile secretion of luteinizing hormone: differential
962 suppression by ovarian steroids. Endocrinology 107:1286-1290.
963 Han SK, Lee K, Bhattarai JP, Herbison AE (2010) Gonadotrophin-releasing hormone (GnRH)
964 exerts stimulatory effects on GnRH neurons in intact adult male and female mice. J
965 Neuroendocrinol 22:188-195.
966 He W, Li X, Adekunbi D, Liu Y, Long H, Wang L, Lyu Q, Kuang Y, O'Byrne KT (2017) Hypothalamic
967 effects of progesterone on regulation of the pulsatile and surge release of luteinising
968 hormone in female rats. Sci Rep 7:8096.
969 Heinrich C, Lähteinen S, Suzuki F, Anne-Marie L, Huber S, Häussler U, Haas C, Larmet Y, Castren
970 E, Depaulis A (2011) Increase in BDNF-mediated TrkB signaling promotes
971 epileptogenesis in a mouse model of mesial temporal lobe epilepsy. Neurobiol Dis
972 42:35-47.
973 Herbison AE (2006) Physiology of the Gonadotropin-Releasing Hormone Neuronal Network. In:
974 Knobil and Neill's Physiology of Reproduction, 3rd Edition (Neill JD, ed), pp 1415-1482.
975 New York: Raven Press.

976 Herzog AG (2008) Disorders of reproduction in patients with epilepsy: primary neurological
977 mechanisms. Seizure 17:101-110.
978 Herzog AG, Klein P, Rand BJ (1997) Three patterns of catamenial epilepsy. Epilepsia 38:1082-
979 1088.
980 Herzog AG, Seibel MM, Schomer DL, Vaitukaitis JL, Geschwind N (1986a) Reproductive
981 endocrine disorders in women with partial seizures of temporal lobe origin. Arch Neurol
982 43:341-346.
983 Herzog AG, Seibel MM, Schomer DL, Vaitukaitis JL, Geschwind N (1986b) Reproductive
984 endocrine disorders in men with partial seizures of temporal lobe origin. Arch Neurol
985 43:347-350.
986 Herzog AG, Drislane FW, Schomer DL, Levesque LA, Ives J, Blume HW, Dubuisson D, Cosgrove
987 GR (1990) Abnormal pulsatile secretion of luteinizing hormone in men with epilepsy:
988 relationship to laterality and nature of paroxysmal discharges. Neurology 40:1557-1561.
989 Herzog AG, Coleman AE, Jacobs AR, Klein P, Friedman MN, Drislane FW, Ransil BJ, Schomer DL
990 (2003) Interictal EEG discharges, reproductive hormones, and menstrual disorders in
991 epilepsy. Ann Neurol 54:625-637.
992 Herzog AG, Harden CL, Liporace J, Pennell P, Schomer DL, Sperling M, Fowler K, Nikolov B,
993 Shuman S, Newman M (2004) Frequency of catamenial seizure exacerbation in women
994 with localization-related epilepsy. Ann Neurol 56:431-434.
995 Hoffman GE, Smith MS, Verbalis JG (1993) c-Fos and related immediate early gene products as
996 markers of activity in neuroendocrine systems. Front Neuroendocrinol 14:173-213.

997 Jasoni CL, Todman MG, Han S-K, Herbison AE (2005) Expression of mRNAs encoding receptors
998 that mediate stress signals in gonadotropin-releasing hormone neurons of the mouse.
999 Neuroendocrinology 82:320-328.
1000 Kalinin VV, Zheleznova EV (2007) Chronology and evolution of temporal lobe epilepsy and
1001 endocrine reproductive dysfunction in women: relationships to side of focus and
1002 catameniality. Epilepsy Behav 11:185-191.
1003 Kelly MJ, Wagner EJ (2002) GnRH neurons and episodic bursting activity. Trends Endocrinol
1004 Metab 13:409-410.
1005 Klein P, Serje A, Pezzullo JC (2001) Premature ovarian failure in women with epilepsy. Epilepsia
1006 42:1584-1589.
1007 Laidlaw J (1956) Catamenial epilepsy. The Lancet 268:1235-1237.
1008 Lawrence C, Martin BS, Sun C, Williamson J, Kapur J (2010) Endogenous neurosteroid synthesis
1009 modulates seizure frequency. Ann Neurol 67:689-693.
1010 Leipheimer RE, Bona-Gallo A, Gallo RV (1984) The influence of progesterone and estradiol on
1011 the acute changes in pulsatile luteinizing hormone release induced by ovariectomy on
1012 diestrus day 1 in the rat. Endocrinology 114:1605-1612.
1013 Li J, Kim JS, Abejuela VA, Lamano JB, Klein NJ, Christian CA (2017) Disrupted female estrous
1014 cyclicity in the intrahippocampal kainic acid mouse model of temporal lobe epilepsy.
1015 Epilepsia Open 2:39-47.
1016 Löfgren E, Mikkonen K, Tolonen U, Pakarinen A, Koivunen R, Myllyla VV, Tapanainen JS, Isojärvi
1017 JI (2007) Reproductive endocrine function in women with epilepsy: the role of epilepsy
1018 type and medication. Epilepsy Behav 10:77-83.

1019 Madisen L, Zwingman TA, Sunkin SM, Oh SW, Zariwala HA, Gu H, Ng LL, Palmiter RD, Hawrylycz
1020 MJ, Jones AR (2010) A robust and high-throughput Cre reporting and characterization
1021 system for the whole mouse brain. Nat Neurosci 13:133-140.
1022 Maguire JL, Stell BM, Rafizadeh M, Mody I (2005) Ovarian cycle–linked changes in GABAA
1023 receptors mediating tonic inhibition alter seizure susceptibility and anxiety. Nat
1024 Neurosci 8:797-804.
1025 Margerison JH, Corsellis JA (1966) Epilepsy and the temporal lobes. A clinical,
1026 electroencephalographic and neuropathological study of the brain in epilepsy, with
1027 particular reference to the temporal lobes. Brain 89:499-530.
1028 Mattis J, Brill J, Evans S, Lerner TN, Davidson TJ, Hyun M, Ramakrishnan C, Deisseroth K,
1029 Huguenard JR (2014) Frequency-dependent, cell type-divergent signaling in the
1030 hippocamposeptal projection. J Neurosci 34:11769-11780.
1031 Meo R, Bilo L, Nappi C, Tommaselli AP, Valentino R, Nocerino C, Striano S, Buscaino GA (1993)
1032 Derangement of the hypothalamic GnRH pulse generator in women with epilepsy.
1033 Seizure 2:241-252.
1034 Moenter SM, Chu Z, Christian CA (2009) Neurobiological Mechanisms Underlying Oestradiol
1035 Negative and Positive Feedback Regulation of Gonadotrophin-Releasing Hormone
1036 Neurones. J Neuroendocrinol 21:327-333.
1037 Moenter SM, DeFazio RA, Pitts GR, Nunemaker CS (2003) Mechanisms underlying episodic
1038 gonadotropin-releasing hormone secretion. Front Neuroendocrinol 24:79-93.
1039 Norberg R, Campbell R, Suter KJ (2013) Ion channels and information processing in GnRH
1040 neuron dendrites. Channels 7:135-145.

1041 Nunemaker CS, DeFazio RA, Moenter SM (2002) Estradiol-sensitive afferents modulate long-
1042 term episodic firing patterns of GnRH neurons. Endocrinology 143:2284-2292.
1043 Paxinos G, Franklin KBJ (2012) The Mouse Brain in Stereotaxic Coordinates, 4th Edition. London:
1044 Elsevier Academic Press.
1045 Pielecka J, Quaynor SD, Moenter SM (2006) Androgens increase gonadotropin-releasing
1046 hormone neuron firing activity in females and interfere with progesterone negative
1047 feedback. Endocrinology 147:1474-1479.
1048 Quigg M, Kiely JM, Shneker B, Veldhuis JD, Bertram EH (2002) Interictal and postictal alterations
1049 of pulsatile secretions of luteinizing hormone in temporal lobe epilepsy in men. Ann
1050 Neurol 51:559-566.
1051 Raedt R, Van Dycke A, Van Melkebeke D, De Smedt T, Claeys P, Wyckhuys T, Vonck K, Wadman
1052 W, Boon P (2009) Seizures in the intrahippocampal kainic acid epilepsy model:
1053 characterization using long-term video-EEG monitoring in the rat. Acta Neurol Scand
1054 119:293-303.
1055 Ramcharan EJ, Gnadt JW, Sherman SM (2000) Burst and tonic firing in thalamic cells of
1056 unanesthetized, behaving monkeys. Vis Neurosci 17:55-62.
1057 Reddy DS, Rogawski MA (2012) Neurosteroids - Endogenous Regulators of Seizure Susceptibility
1058 and Role in the Treatment of Epilepsy. In: Jasper's Basic Mechanisms of the Epilepsies
1059 (Noebels JL, Avoli M, Rogawski MA, Olsen RW, Delgado-Escueta AV, eds). Bethesda (MD):
1060 National Center for Biotechnology Information (US).

1061 Riban V, Bouilleret V, Pham-Le B, Fritschy J-M, Marescaux C, Depaulis A (2002) Evolution of
1062 hippocampal epileptic activity during the development of hippocampal sclerosis in a
1063 mouse model of temporal lobe epilepsy. Neuroscience 112:101-111.
1064 Runtz L, Girard B, Toussenot M, Espallergues J, Fayd'Herbe De Maudave A, Milman A, deBock F,
1065 Ghosh C, Guerineau NC, Pascussi JM, Bertaso F, Marchi N (2018) Hepatic and
1066 hippocampal cytochrome P450 enzyme overexpression during spontaneous recurrent
1067 seizures. Epilepsia 59:123-134.
1068 Sarkar DK, Fink G (1980) Luteinizing hormone releasing factor in pituitary stalk plasma from
1069 long-term ovariectomized rats: effects of steroids. J Endocrinol 86:511-524.
1070 Scharfman HE, Kim M, Hintz TM, MacLusky NJ (2008) Seizures and reproductive function:
1071 insights from female rats with epilepsy. Ann Neurol 64:687-697.
1072 Sheybani L, Birot G, Contestabile A, Seeck M, Kiss JZ, Schaller K, Michel CM, Quairiaux C (2018)
1073 Electrophysiological Evidence for the Development of a Self-Sustained Large-Scale
1074 Epileptic Network in the Kainate Mouse Model of Temporal Lobe Epilepsy. J Neurosci
1075 38:3776-3791.
1076 Smith MA, Perrin MH, Vale WW (1983) Desensitization of cultured pituitary cells to
1077 gonadotropin-releasing hormone: evidence for a post-receptor mechanism. Mol Cell
1078 Endocrinol 30:85-96.
1079 Sullivan SD, Moenter SM (2005) GABAergic integration of progesterone and androgen feedback
1080 to gonadotropin-releasing hormone neurons. Biol Reprod 72:33-41.
1081 Talbot JA, Sheldrick R, Caswell H, Duncan S (2008) Sexual function in men with epilepsy How
1082 important is testosterone? Neurology 70:1346-1352.

1083 Terasawa E, Kawakami M (1973) Effects of limbic forebrain ablation on pituitary gonadal
1084 function in the female rat. Endocrinol Jpn 20:277-289.
1085 Todman MG, Han SK, Herbison AE (2005) Profiling neurotransmitter receptor expression in
1086 mouse gonadotropin-releasing hormone neurons using green fluorescent protein-
1087 promoter transgenics and microarrays. Neuroscience 132:703-712.
1088 Velasco ME, Taleisnik S (1969) Effect of hippocampal stimulation on the release of
1089 gonadotropin. Endocrinology 85:1154-1159.
1090 Wakerley JB, Lincoln DW (1973) The milk-ejection reflex of the rat: a 20- to 40-fold acceleration
1091 in the firing of paraventricular neurones during oxytocin release. J Endocrinol 57:477-
1092 493.
1093 Wildt L, Hausler A, Marshall G, Hutchison JS, Plant TM, Belchetz PE, Knobil E (1981) Frequency
1094 and amplitude of gonadotropin-releasing hormone stimulation and gonadotropin
1095 secretion in the rhesus monkey. Endocrinology 109:376-385.
1096 Wintermantel TM, Campbell RE, Porteous R, Bock D, Grone HJ, Todman MG, Korach KS, Greiner
1097 E, Perez CA, Schutz G, Herbison AE (2006) Definition of estrogen receptor pathway
1098 critical for estrogen positive feedback to gonadotropin-releasing hormone neurons and
1099 fertility. Neuron 52:271-280.
1100 Xu C, Xu XZ, Nunemaker CS, Moenter SM (2004) Dose-dependent switch in response of
1101 gonadotropin-releasing hormone (GnRH) neurons to GnRH mediated through the type I
1102 GnRH receptor. Endocrinology 145:728-735.
1103 Yoon H, Enquist L, Dulac C (2005) Olfactory inputs to hypothalamic neurons controlling
1104 reproduction and fertility. Cell 123:669-682.

1105 Zhou J-Q, Zhou L-M, Chen L-J, Han J-D, Wang Q, Fang Z-Y, Chen Z-Y, Ling S (2012) Polycystic
1106 ovary syndrome in patients with epilepsy: a study in 102 Chinese women. Seizure
1107 21:729-733.

1108

1109

Figure Legends

Figure 1. Experimental design and timeline. Paradigm of test groups, procedures, and experimental time points. Procedures exclusive to experiments in females are marked in red.

Figure 2. **Verification of KA injection targeting. A**. Example Cresyl Violet staining from a KA-regular female with marked granule cell dispersion ipsilateral to the injection, and intact hippocampus contralateral to the injection. **B**. Cresyl Violet (top) and GFAP/DAPI staining (bottom) from a KA-regular female. Note the strong GFAP immunoreactivity in the injected hippocampus, despite absence of major pathology observed in Cresyl Violet staining of adjacent sections. GFAP = green, DAPI = blue. Left: ipsilateral to the injection. **C.** Example GFAP staining in tissue from a saline-injected mouse. Scale bar: 500 μm. Black arrow: hippocampal sclerosis detected by Cresyl Violet stain. White arrows: gliosis in CA and dentate gyrus detected by GFAP staining.

Figure 3. **Diestrus vs. estrus shifts in GnRH neuron mean firing rate are compromised in the intrahippocampal KA mouse model of TLE. A**. Example raw traces of bursts (top) and individual (bottom) action currents detected in loose patch recordings. **B**. Representative raster plots of activity in GnRH neurons from control and KA-injected females. The black arrow marks the end of recording. The mean firing rate of each cell is given in parentheses. **C.** Mean ± SEM for GnRH neuron firing rate in control (open bars), KA-long (red bars), and KA-regular (blue bars) groups. KA-injected females are divided into KA-long and KA-regular groups based on their estrous cycle

length (KA-long ≥7 d, KA-regular 4-6 d). Cells were recorded on diestrus (left) or estrus (right). **D**. Firing rates in individual cells, plotted on a logarithmic scale to show the full range. **E**. Correlation analyses between GnRH neuron firing rate and estrous cycle length in KA-injected females performed with data combined from KA-long (red circles) and KA-regular groups (blue circles). Black line: line of best fit for all points. **F-G.** Comparison of GnRH neuron firing rate between controls, KA-long, and KA-regular groups based on anatomical location of somata for cells recorded on diestrus (F) or estrus (G). Data are shown as group mean firing rates (top, mean ± SEM) and individual neuron firing rates (bottom). MS: medial septum. POA: preoptic area. AHA: anterior hypothalamic area. *p<0.05, **p<0.01 for comparisons between saline, KA-long, and KA-regular females by Kruskal-Wallis with Dunn's *post hoc* tests. $^{\#}$p<0.05, $^{\#\#}$p<0.01 for comparisons between diestrus and estrus within groups by t-tests or Mann-Whitney tests. In scatter plots of individual neuron firing rate, neurons plotted below y = 0.01 showed firing rates ≥0 Hz and below 0.01 Hz.

Figure 4. GnRH neuron firing patterns are altered in KA-injected female mice on both diestrus and estrus. A-B. Examples of burst detection and firing pattern categorization. **A.** Left: example ISI joint scatter plot with a randomly selected candidate burst ISI threshold value (red line). The four quadrants divide all data into four clusters: C1, C2, C3, and C4. Right: example ISI Threshold Validation shows the summed distance for each candidate burst ISI threshold value. The summed distance is calculated by the summation of squared distance between every point and its corresponding cluster centroid. The candidate value with the smallest summed distance is chosen as the optimal burst ISI threshold. **B.** Examples of scatter plots for GnRH neuron

bursting (left), irregular spiking (middle) and tonic spiking (right) patterns. The different colors represent the final C1 to C4 distribution with the optimal burst ISI threshold for each cell. Black circles: individual centroids of clusters C1 – C4. **C.** Proportion of GnRH neurons from female mice categorized into each pattern on diestrus (left) and estrus (right). *p<0.05 for pair-wise Fisher's exact test comparisons for indicated firing pattern between control and KA-injected groups. #p<0.05 for comparisons for indicated firing pattern between diestrus and estrus within control and KA-injected groups. Δ, p<0.05 for comparisons for indicated firing pattern between KA-long and KA-regular groups within the same estrous cycle stage.

Figure 5. GnRH neuron burst properties on diestrus and estrus; only neurons displaying burst spiking patterns were used for comparisons. A. Cumulative probability distributions for burst properties of GnRH neurons from control female mice on diestrus (gray traces) and estrus (purple traces). Cumulative distributions were constructed using 100 randomly selected bursts per cell. **B.** Burst properties from KA-long female mice. **C.** Burst properties from KA-regular female mice. **p<0.0001 for comparisons by Kolmogorov–Smirnov tests. n.s. = not significant. The interburst intervals are presented on logarithmic scales for better visualization of the major portion (1% to 99%) of the distributions.

Figure 6. Bursting GnRH neurons from KA-injected female mice show changed burst properties. A. Cumulative probability distributions for burst properties in cells displaying bursting patterns from controls (black traces), KA-long (red traces), and KA-regular (blue traces)

1174 mice recorded on diestrus. Cumulative distributions were constructed using 100 randomly
1175 selected bursts per cell. **B.** Cumulative probability distributions for burst properties recorded on
1176 estrus. **p<0.01 for comparisons between saline, KA-long, or KA-regular by pairwise
1177 Kolmogorov–Smirnov tests. n.s. = not significant. The interburst intervals are presented on
1178 logarithmic scales for better visualization of the major portion (1% to 99%) of the distributions.

1179

1180 **Figure 7. GnRH neuron intrinsic excitability is elevated on both diestrus and estrus in the**
1181 **intrahippocampal KA mouse model of TLE. A.** Representative examples of evoked firing in
1182 response to depolarizing current steps in cells recorded on diestrus (left) and estrus (right). The
1183 KA traces are offset to highlight differences in spiking. All traces started from a membrane
1184 potential of approximately -73 mV, corrected for the liquid junction potential. **B.** Frequency-
1185 current (F-I) curves for GnRH neurons recorded on diestrus (left) or estrus (right), classified by
1186 the location of the somata of recorded neurons. Depolarizing current steps were applied in
1187 increments of 10 pA. *p<0.05 for comparisons of area under the curve by three-way ANOVA
1188 with Fisher's LSD. **C.** Mean ± SEM for area under the curve of evoked firing rate plots on diestrus
1189 and estrus in cells from control (black symbols and line), KA-long (red symbols and line), and KA-
1190 regular (blue symbols and line) mice. **D.** Mean ± SEM for action potential threshold, membrane
1191 time constant (Tau), and Input resistance. *p<0.05, **p<0.01 by two-way ANOVA with Fisher's
1192 LSD; #p<0.05 for comparisons between diestrus and estrus within groups by three-way ANOVA
1193 with Fisher's LSD.

1194

Figure 8. Changes in circulating P_4 and E_2 levels on diestrus and estrus as measured 2 months after KA injection. A. Mean ± SEM for P_4 levels on diestrus (left) and estrus (right) in control (open bars), KA-long (red bars), and KA-regular (blue bars) mice. **B.** Mean ± SEM for E_2 levels on diestrus (left) and estrus (right). *p<0.05 for comparisons between saline, KA-long, and KA-regular groups by one-way ANOVA and Fisher *post hoc* tests. #p<0.05 for comparisons between estrus and diestrus within groups by t-tests.

Figure 9. Impacts of KA-injection on GnRH neuron mean firing rate and excitability in male mice depend on soma location. A. Mean ± SEM for mean firing rate (left) and firing rates for individual GnRH neurons (right) from males treated with saline (open bars and circles) or KA (green bars and circles). **B.** Mean ± SEM for mean firing rate of GnRH neurons from control and KA-injected males classified by soma location. MS: medial septum. POA: preoptic area. AHA: anterior hypothalamic area. *p<0.05, two-sample t-test. **C.** Cumulative probability distributions for burst duration, number of spikes per burst, intraburst firing rate, and interburst intervals in cells from control and KA-injected males. **p<0.0001 by Kolmogorov–Smirnov tests. **D.** F-I curves for GnRH neurons from control and KA-injected males. *p<0.05 for comparison of area under the curve by two-way ANOVA with Fisher's LSD *post hoc* tests. **E.** Mean ± SEM for serum T in control and KA-injected male mice.

Table Legends

Table 1. Outcomes of video screening of acute seizures and hippocampal histology to verify KA injection targeting. Number of seizures refers to behavioral seizures Racine stage 3 or higher observed within 5 hours of KA injection. Hippocampal tissue from mice that either did not show acute seizures or for whom videos were not available was collected ~2 months after KA injection. Sclerosis was assessed via Cresyl Violet (Nissl) staining. Sections of hippocampi that did not display signs of sclerosis were further assessed for gliosis via GFAP staining. *= mouse removed from dataset in absence of either video confirmation of acute seizure induction or later development of hippocampal sclerosis/gliosis.

Table 2. Effects of KA injection, estrous cycle stage, or an interaction between KA injection and cycle stage on probability of occurrence of each firing pattern in logistic regression analysis. P-values from logistic regressions performed for each firing pattern. *p<0.05, **p<0.01, ***p<0.001

Table 3. GnRH neuron excitability parameters and action potential kinetics for each treatment and cycle stage in females. ISI first 10 Spikes: average interspike interval of the first 10 evoked spikes. Ins. freq. first 10 spikes: average instantaneous frequency of the first 10 evoked spikes. FWHM: full-width at half-maximum. AHP: afterhyperpolarization. Time to AHP: time between the action potential initiation and the peak of AHP. *p<0.05, **p<0.01 two-way ANOVA with Fisher's LSD *post hoc* tests

Table 4. GnRH neuron excitability parameters and action potential kinetics for saline and KA-injected males. ISI first 10 Spikes: average interspike interval of the first 10 evoked spikes. Ins. freq. first 10 spikes: average instantaneous frequency of the first 10 evoked spikes. FWHM: full-width at half-maximum. AHP: afterhyperpolarization. Time to AHP: time between the action potential initiation and the peak of AHP. Two-sample t-tests for each parameter did not identify any differences between controls and KA-injected groups.

Extended Data 1. GnRH Neuron Firing Pattern and Burst Properties Analyzer. This code was created in MATLAB R2015b running in a Windows 10 operating system. Run PlotBursts.m in MATLAB to generate the ISI scatter plot, find the optimal burst ISI threshold, view the ratio of data points between quadrants in the scatter plot, generate cumulative probability plots of the examined burst properties, and execute Kolmogorov–Smirnov comparisons of the probability plots. Example data from two GnRH neurons (saline-injected females, diestrus & estrus) are provided for demonstration purposes. The code is written to analyze raw data containing neuron spike times in the .mat format. More details are available in the README file and documentation within the script.

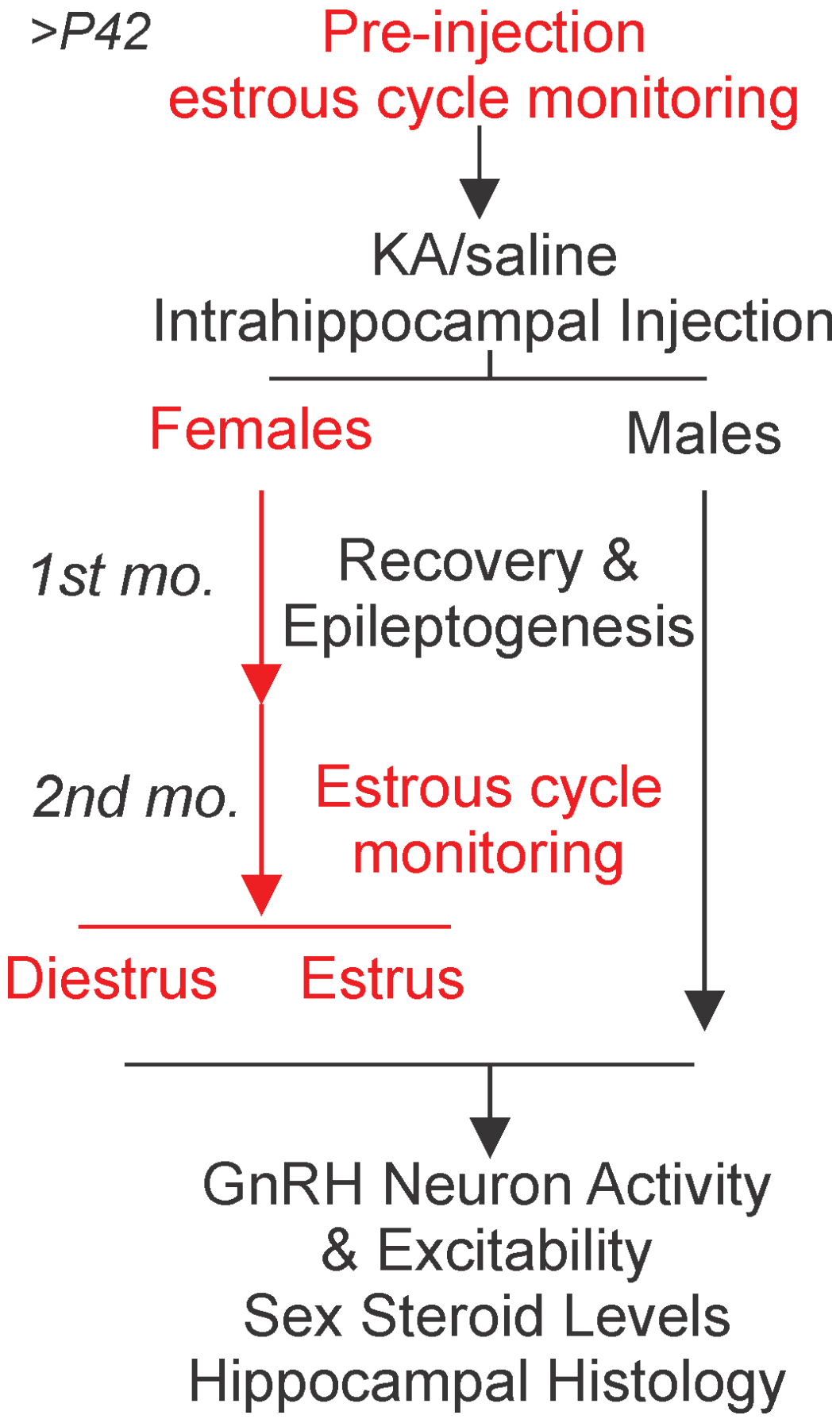

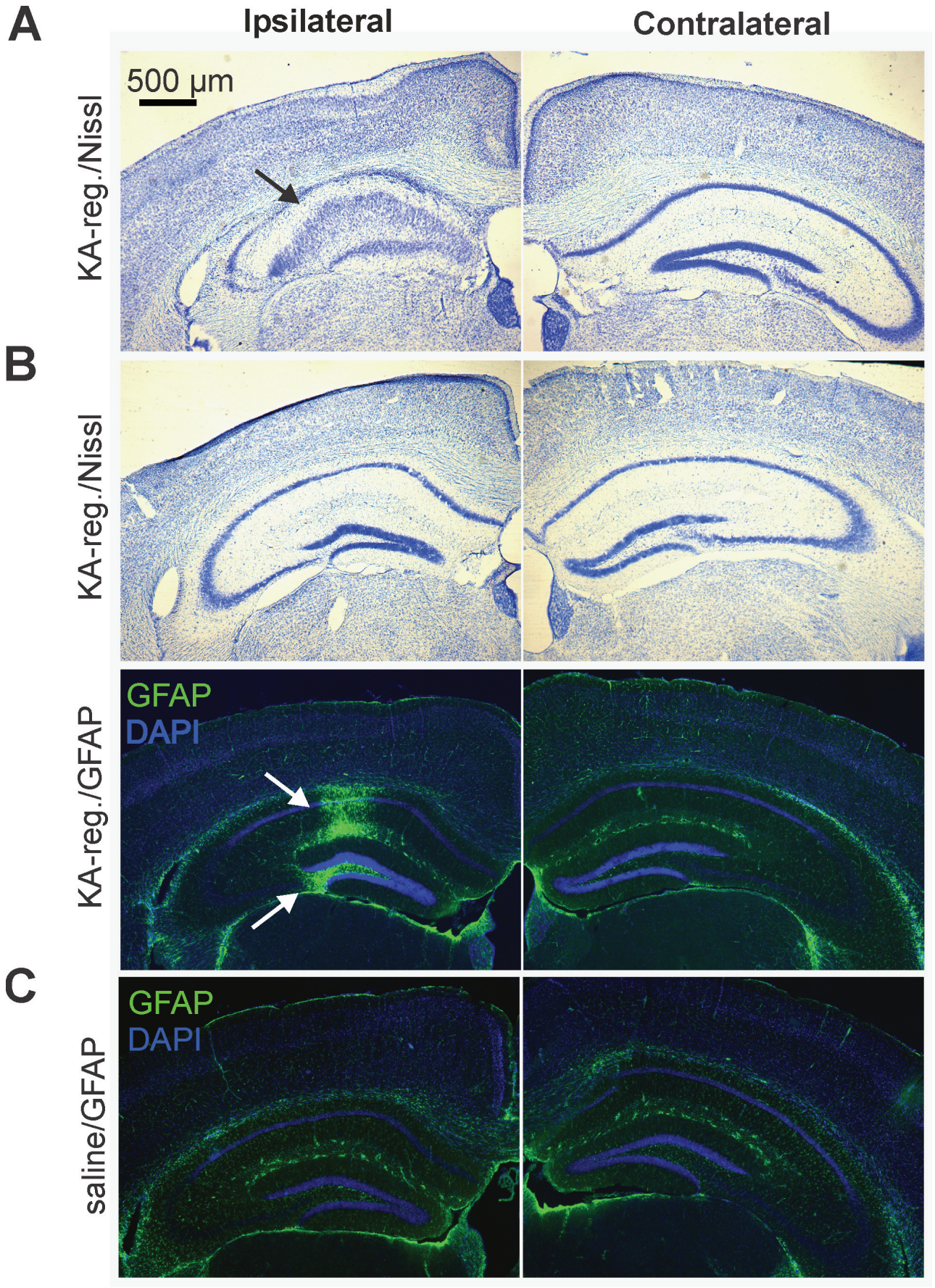

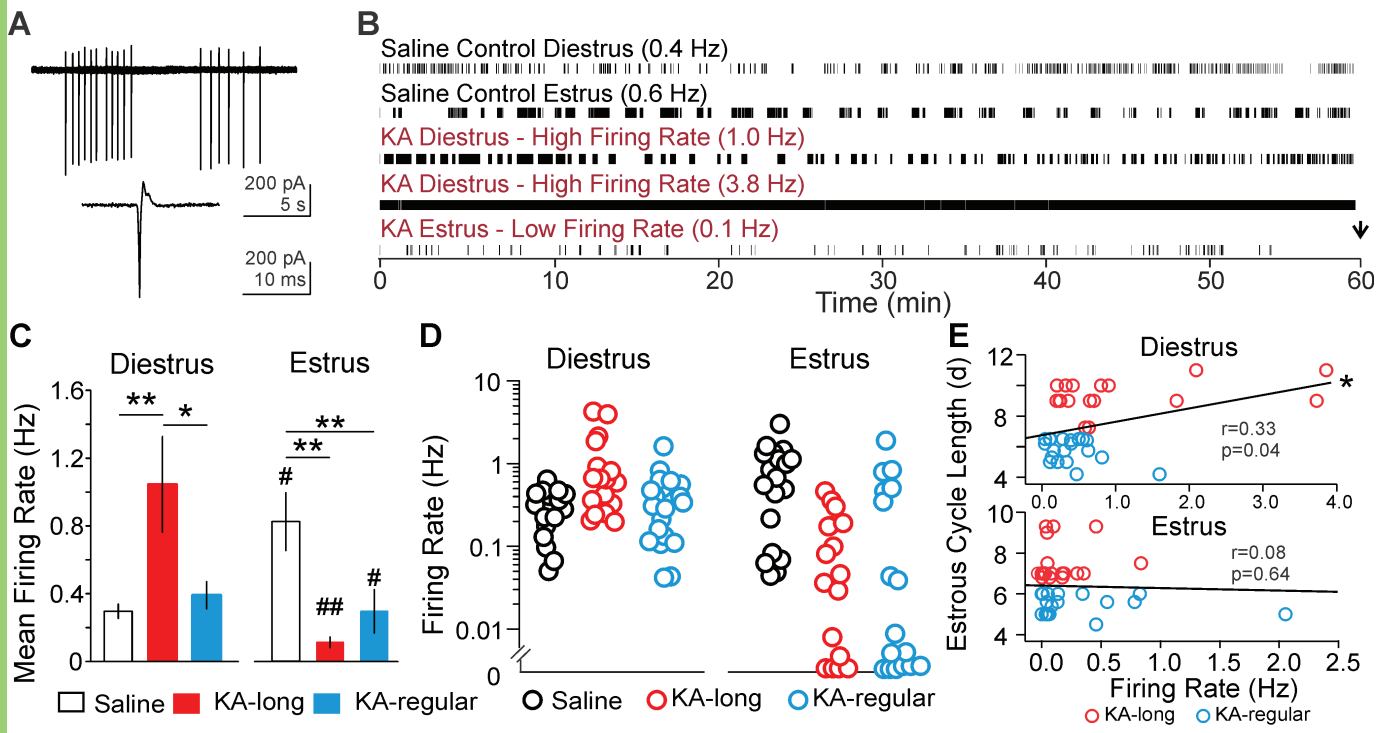

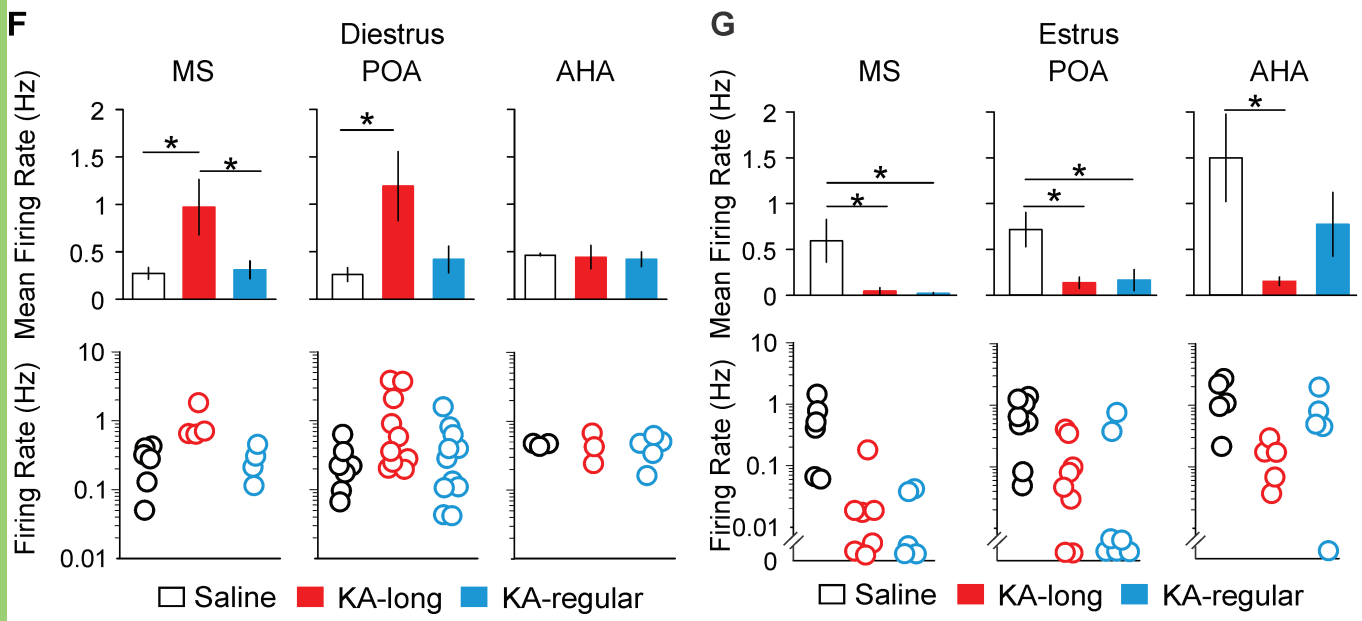

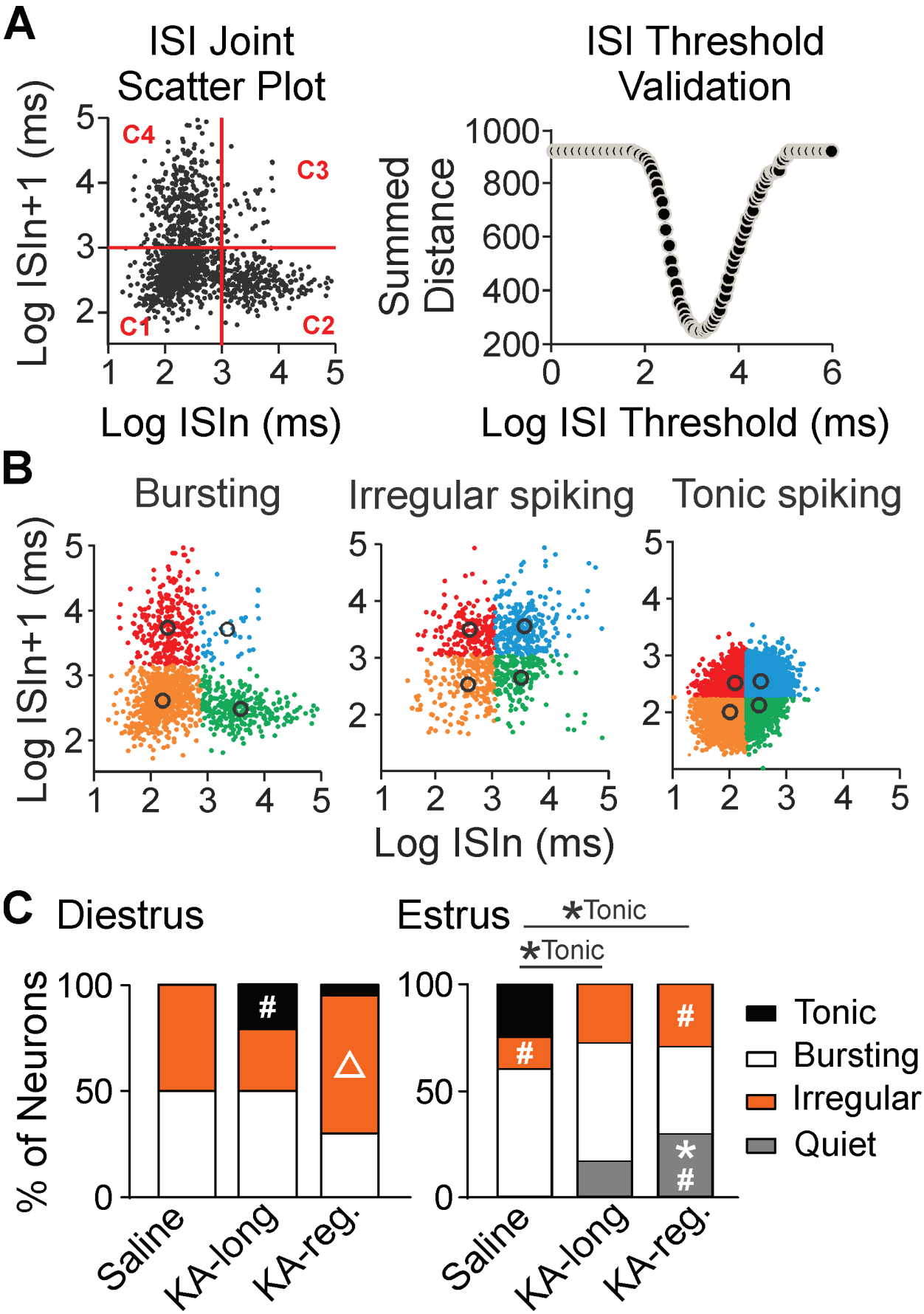

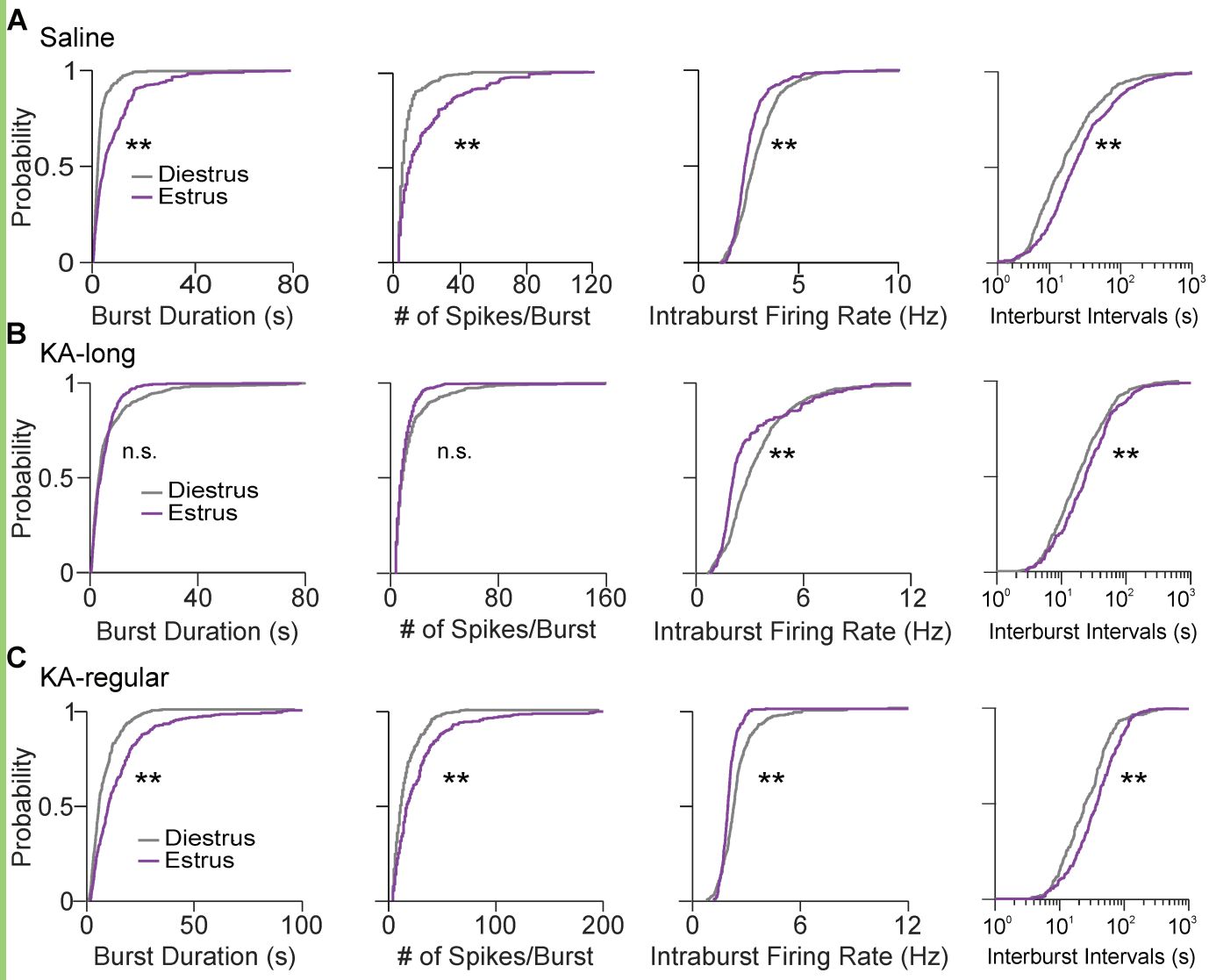

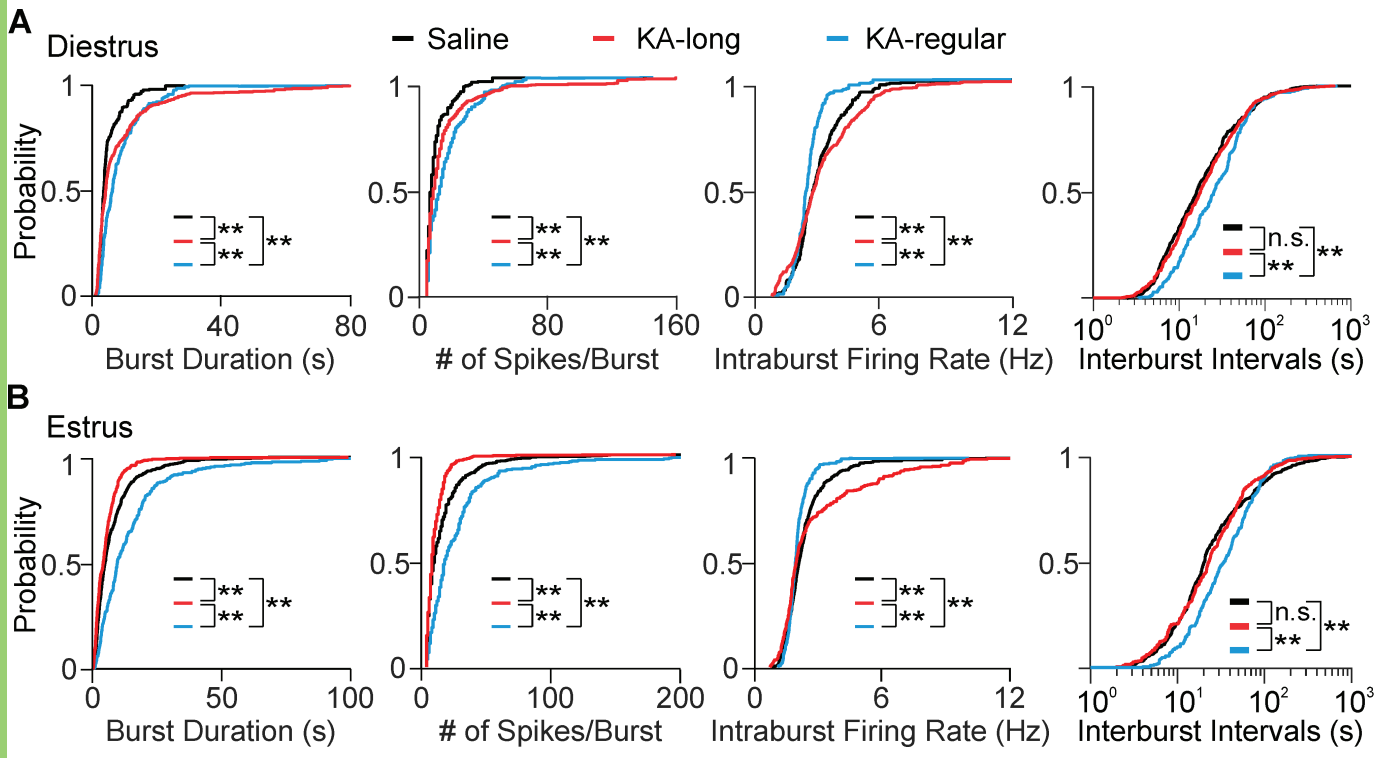

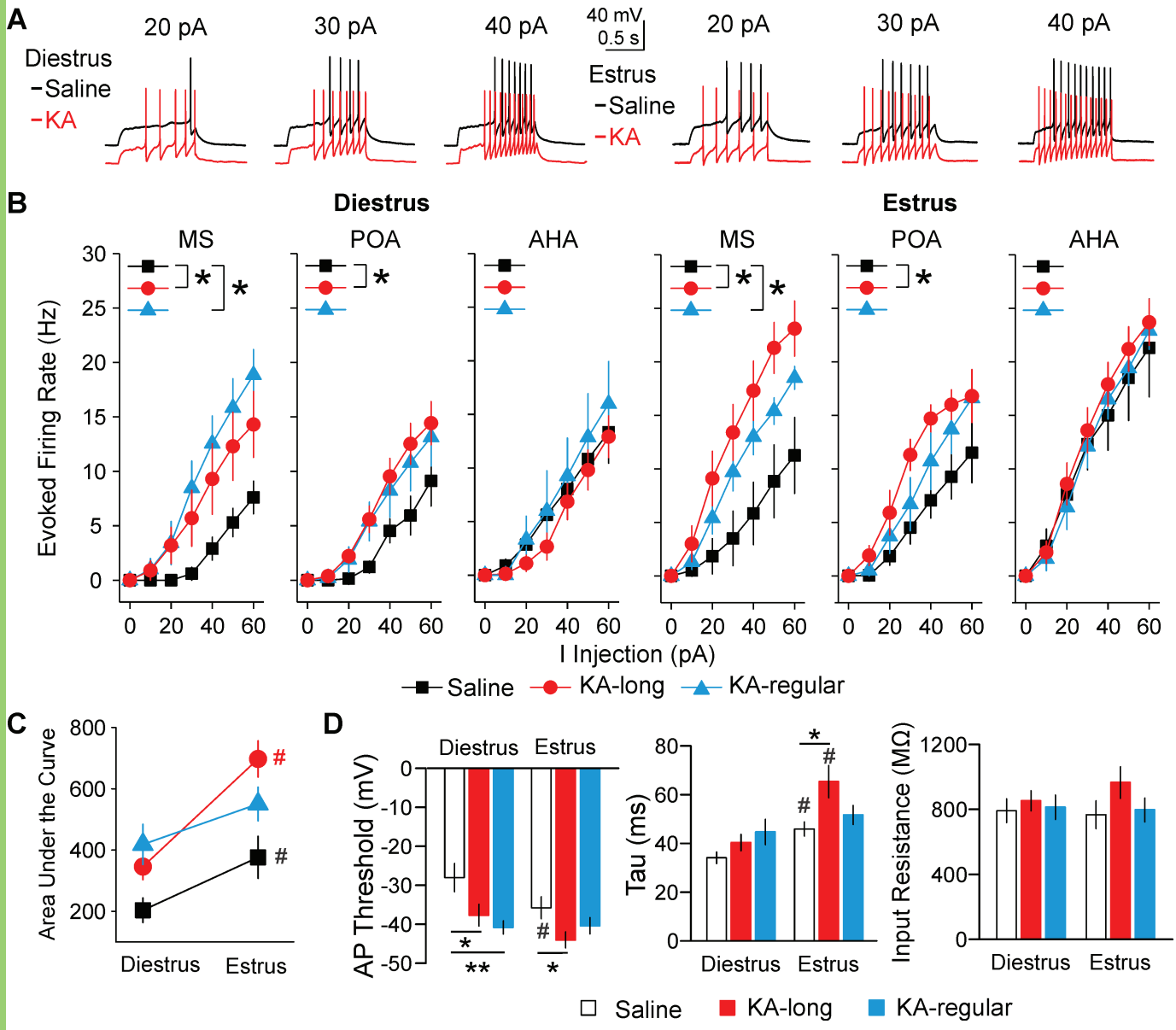

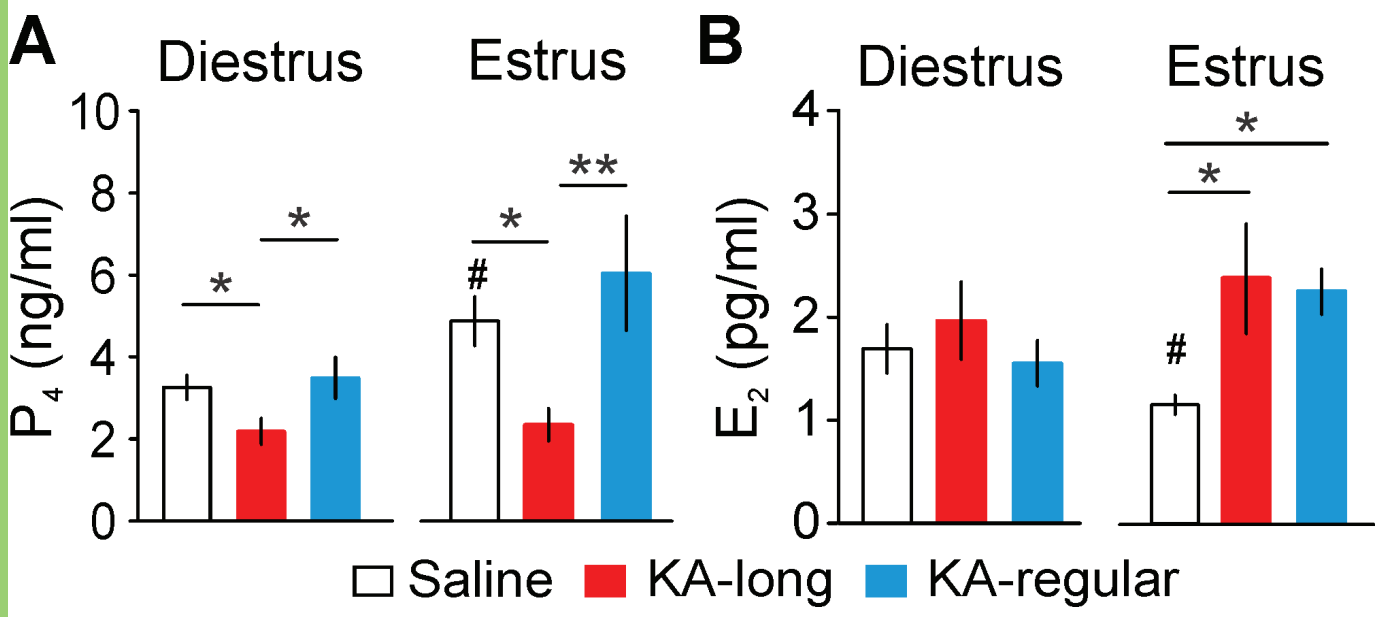

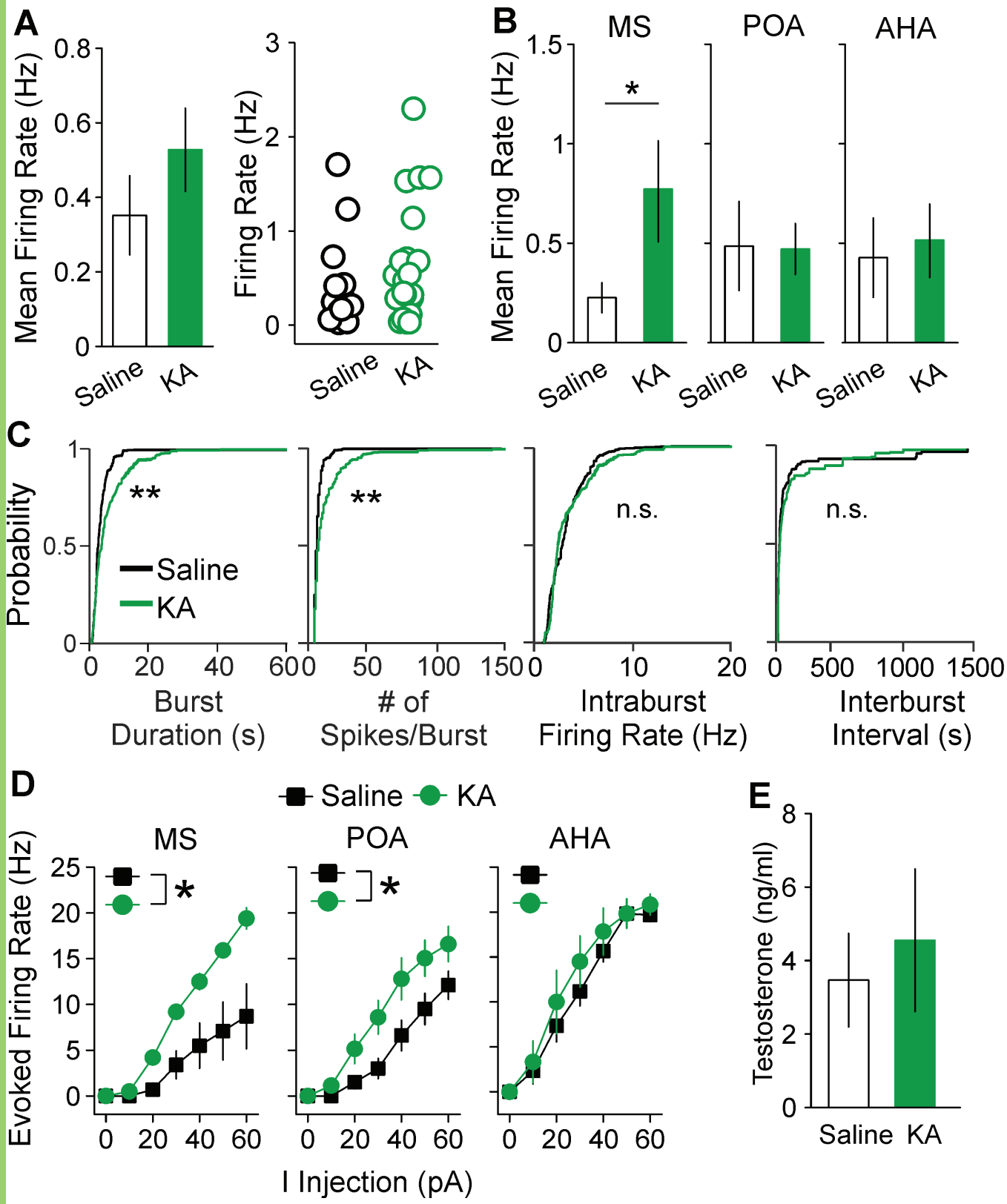

Table 1

Outcomes of video screening of acute seizures and hippocampal histology to verify KA injection targeting

Video screening outcome (acute seizures)				
	> 2 seizures	1 seizure	No seizures or video	Total
Females	57	5	7	69
Males	10	0	5	15
Histology for mice with no seizures or video (2 months post-KA injection)				
	Sclerosis	Gliosis	No sclerosis or gliosis	Total
Females	4	2	1*	7
Males	5	0	0	5

Table 2

Effects of KA injection, estrous cycle stage, or an interaction between KA injection and cycle stage on probability of occurrence of each firing pattern in logistic regression analysis

Firing pattern	KA injection	Cycle stage	Interaction of KA injection and cycle stage
Tonic	0.17	0.84	0.0009***
Bursting	0.18	0.30	0.99
Irregular	0.15	0.0072**	0.25
Quiet	0.027*	0.0003***	1.00

Table 3

Effects of KA treatment or estrous cycle stage on GnRH neuron excitability parameters and action potential kinetics in females

Parameters	Diestrus			Estrus			Overall ANOVA (F value)	
	Saline	KA-long	KA-reg.	Saline	KA-long	KA-reg.	Treatment	Cycle Stage
AP threshold (mV)	-28 ± 3.6	-39.1 ± 2.5*	-40.8 ± 1.7**	-35.8 ± 2.8$^{\#}$	-44.0 ± 2.0*	-40.4 ± 2.1	6.57*	4.54*
Input resistance (MΩ)	791.5 ± 73.0	852.3 ± 62.3	812.8 ± 75.3	766.8 ± 85.9	965.0 ± 97.1	796.0 ± 73.1	1.37	0.43
Capacitance (pF)	18.5 ± 2.7	14.8 ± 0.7	16.5 ± 1.6	17.9 ± 2.0	16.1 ± 0.8	18.5 ± 1.1	0.63	1.21
Tau (ms)	34.1 ± 2.4	40.4 ± 3.4	44.7 ± 5.2	45.9 ± 2.9$^{\#}$	65.3 ± 6.6*$^{\#}$	51.7 ± 3.9	4.45*	17.02**
Latency to firing (ms)	0.57 ± 0.07	0.47 ± 0.05	0.48 ± 0.08	0.50 ± 0.07	0.36 ± 0.08*	0.43 ± 0.06	1.66	2.40
ISI first 10 Spikes (ms)	10.0 ± 0.3	9.1 ± 0.2	9.6 ± 0.4	9.1 ± 0.4	9.8 ± 0.5	9.2 ± 0.3	2.71	0.50
Ins. freq. first 10 spikes (Hz)	112.9 ± 6.1	122.3 ± 4.1	117.9 ± 6.0	130.3 ± 7.2	113.8 ± 5.7	119.8 ± 5.1	0.10	0.50
FWHM (ms)	2.1 ± 0.1	2.2 ± 0.1	2.3 ± 0.2	2.4 ± 0.1	2.5 ± 0.2	2.4 ± 0.1	0.99	0.43
AHP (pA)	35.0 ± 3.2	29.7 ± 2.0	27.9 ± 1.8	30.2 ± 1.4	28.7 ± 2.0	27.9 ± 2.0	2.52	0.33
Time to AHP (ms)	3.8 ± 0.1	3.8 ± 0.1	3.7 ± 0.2	4.1 ± 0.2	3.9 ± 0.3	3.8 ± 0.3	0.19	0.76
Max rise slope	171.3 ± 11.7	182.7 ± 12.6	155.8 ± 14.4	155.5 ± 12.2	157.1 ± 13.0	163.1 ± 15.4	0.58	1.66
Max decay slope	-80.9 ± 3.7	-78.8 ± 4.2	-67.4 ± 6.5	-74.8 ± 3.8	-71.9 ± 3.4	-73.2 ± 3.8	1.94	0.88

Table 4

GnRH neuron excitability parameters and action potential kinetics for saline and KA-injected males

Parameters	Saline	KA
AP threshold (mV)	-40.6 ± 2.9	-42.3 ± 2.3
Input resistance (MΩ)	745.6 ± 36.9	1892.2 ± 984.2
Capacitance (pF)	16.7 ± 1.0	15.7 ± 1.0
Tau (ms)	51.0 ± 3.7	61.7 ± 6.5
Latency to firing (ms)	628.1 ± 67.2	493.5 ± 68.6
ISI first 10 spikes (ms)	123.4 ± 5.4	121.4 ± 3.7
Ins. freq. first 10 spikes (Hz)	9.9 ± 1.2	9.9 ± 0.5
FWHM (ms)	2.3 ± 0.12	2.4 ± 0.3
AHP	31.6 ± 2.6	32.8 ± 1.9
Time to AHP	3.6 ± 0.1	3.5 ± 0.2
Max rise slope	187.3 ± 11.7	158.9 ± 3.2
Max decay slope	-77.5 ± 5.1	-75.3 ± 4.2